Heat induced male meiotic restitution and sexual polyploidisation through natural variation of the Arabidopsis cyclin TAM/CYCA1;2

Short Title: TAM involved in heat induced meiotic restitution

Authors: Cédric Schindfessel[1], Chunlian Jin[1#], Danny Geelen[1*]

[1] Department of Plants and Crops, unit HortiCell, Faculty of Bioscience Engineering, Ghent University, Coupure Links 653, 9000 Ghent, Belgium.

[#] Current affiliation: National Engineering Research Center for Ornamental Horticulture, Key Laboratory for Flower Breeding of Yunnan Province, Floriculture Research Institute, Yunnan Academy of Agricultural Science, Kunming, China.

*corresponding author: danny.geelen@ugent.be

The author responsible for distribution of materials integral to the findings presented in this article in accordance with the policy described in the Instructions for Authors (https://academic.oup.com/plcell/pages/General-Instructions) is: Danny Geelen (danny.geelen@ugent.be)

ABSTRACT

High temperature stress has a profound impact on many aspects of plant development. Particularly male germline development is highly sensitive and has received extensive attention in the light of the ongoing climate change. We here uncover a major role for the cyclin TAM/CYCA1;2 in heat induced male meiotic restitution. By exploiting natural variation in Arabidopsis thaliana we identified rare allelic variants of TAM that confer hypersensitivity to heat stress. The increase of the ambient temperature to 32°C for 24 hours is sufficient to stimulate the production of up to 100% unreduced meiocytes, resulting in sexual polyploidisation. Arabidopsis accessions with a heat sensitive TAM allele show elevated expression of TAM at 32°C and overexpression of TAM phenocopies the meiotic restitution phenotype of a TAM knock-out. These results are discussed in terms of the molecular mechanism and indicate a critical role for meiotic cell cycle regulation in sexual polyploidization and plant evolutionary processes.

INTRODUCTION

Meiosis is a highly conserved process in sexually reproducing organisms. The cycle of DNA duplication, followed by a double division before fusion of the male and female gametes ensures ploidy stability of a species. At the same time, the process of meiotic recombination during prophase I and the subsequent segregation of the chromatids allow for genetic variation by reshuffling the parental genomes (Osman et al. 2011; Mercier et al. 2015; Wang and Copenhaver 2018). Of great interest to researchers and breeders is the fact that this seemingly rigid process can show great flexibility in response to environmental stimuli (De Storme and Geelen 2014; Younis et al. 2014; Bomblies et al. 2015; Modliszewski and Copenhaver 2017). In the light of the ongoing climate change, particularly the influence of different environmental temperatures on the meiotic process and plant fertility in general has received much attention (Zinn et al. 2010; Mittler et al. 2012; Giorno et al. 2013; Bac-Molenaar et al. 2015; Rieu et al. 2017). Research has mainly focused on the male gametophyte, due to the higher sensitivity compared to the female gametophyte (Zinn et al. 2010; Chaturvedi et al. 2021) and the abundance and ease of access of microspores and pollen compared to egg cells.

Male meiotic restitution, whereby either the first or second meiotic division is omitted (Brownfield and Köhler 2011; De Storme and Geelen 2013), is observed frequently as a consequence of (high) temperature stress in both monocot and dicot species (Pécrix et al. 2011; Omidi et al. 2014; Wang et al. 2017; De Storme and Geelen 2020; Schindfessel et al. 2021). The subsequent production of unreduced gametes with the diploid (2n) instead of the haploid (n) chromosome number is a major driver of polyploidisation in plants (Bretagnolle and Thompson 1995), and is likely enhanced under adverse environmental conditions (Bomblies et al. 2015; Novikova et al. 2018; Fox et al. 2020; Van de Peer et al. 2021).

Male meiotic restitution occurs when meiotic progression is defective and is linked with mutations in TAM/CYCA1;2 (Magnard et al. 2001; Wang et al. 2004), OSD1 (d'Erfurth et al. 2009), TDM1 (Cifuentes et al. 2016) and CDKA;1+CDKD;3 (Sofroni et al. 2020). In these mutants, the complex regulatory network coordinating the progression through male meiosis that also involves SMG7 is deregulated and causes a premature exit after the first meiotic division (Bulankova et al. 2010; d'Erfurth et al. 2010; Cromer et al. 2012). Alternatively, meiotic restitution results from defects in chromosome segregation as observed in mutants of

JASON, atPS1, DUET/MMD1 and AFH14 that regulate, separately or in combination, the organisation and orientation of the meiotic spindles (d'Erfurth et al. 2008; Li et al. 2010; De Storme and Geelen 2011; Andreuzza et al. 2015; Brownfield et al. 2015). In these mutants, meiosis I proceeds into meiosis II and during the second meiotic division parallel or fused spindles form re-joining the sister chromatids from the homologous chromosome pairs. Meiotic restitution is not exclusively caused by a segregation defect in the second division as recently was shown that mutations in the SMC5/6 complex can lead to unreduced gamete production through chromosome segregation defects in both meiosis I and II (Yang et al. 2021).

Although heat induced meiotic restitution has been extensively reported in several natural plant species and the underlying molecular mechanisms described, a molecular link between temperature stress and meiotic restitution has not been reported before. In search for genetic factors contributing to temperature stress induced meiotic restitution, we screened a collection of natural Arabidopsis thaliana accessions and found that allelic variation in TAM is a major component driving natural sexual polyploidization.

RESULTS

Natural variation in heat induced meiotic restitution in Arabidopsis

Arabidopsis thaliana accessions (212 lines) were exposed to 32°C for 24h and compared to a 20°C control. Immediately after this heat treatment, tetrad-stage microspores were visualised under a microscope. The formation of dyads, triads and polyads was recorded to determine the incidence of defects in male meiosis under high temperature stress.

After data curation (see Methods), 172 accessions were retained for further analysis (Supp. File 1). Across these accessions grown under control conditions (20°C), a total of 2 dyads and 1 triad were recorded among 44405 tetrad-stage configurations viewed. All other microspores appeared as tetrads, showing that male meiosis robustly results in 4 haploid microspores at the end of meiosis in a wide variety of Arabidopsis thaliana accessions. After heat treatment a total of 8174 dyads, 1411 triads and otherwise tetrads were recorded out of 84975 microspores, indicating that meiotic restitution as a response to changing environmental temperature is a widespread phenomenon in Arabidopsis. Remarkably, the dyad production

after heat varied largely between accessions, with average dyad production ranging from 0% to nearly 100% (Figure 1a). Overall, the heat-induced dyad production data is zero-inflated, with many accessions producing none or a very low percentage of dyads and only few accessions being highly sensitive (11/172 produce more than 1/3 dyads on average). Plotting the dyad frequency after heat for every accession on a world map revealed no obvious spatial pattern (Figure 1b), indicating there is no direct link between high rates of meiotic restitution and the accessions' geographical location. To determine underlying genetic factors involved in heat induced restitution, the high dyad producing accessions Mt-0 was selected for detailed analyses.

Accession Mt-0 as a model for high dyad production after heat

Under control conditions (20°C) Mt-0 produces microspores organized in a tetrahedral configuration (100%, n=500), and surrounded by callose walls (Figure 2a, d & h). However, after a short heat treatment of 24h at 32°C, tetrad-stage flowerbuds mainly yielded dyads (81.2%, n = 2801), a minor fraction of triads (1.4%) and otherwise tetrads (17.4%) (Figure 2b, c, e, f & h). These dyads appeared balanced (i.e., both microspores appear equal in size and thus likely contain the same number of chromosomes), indicative for problems in cell wall formation, cytokinesis, or an arrest of the first or second meiotic division. Furthermore, callose walls separating and surrounding the microspores in a dyad configuration appeared thin and fragile in aniline blue stainings (in 25/34 dyads) (Figure 2f, Supp. Table S1). Visual inspection of the dyad configurations produced by other high dyad producing accessions revealed subtle histological differences (Supp. Figure S1 and Supp. Tables S1, S2 and S3). These included differences in the thickness of the callose wall separating the microspores (thin vs sturdy), differences in the number of nuclei in each microspore (1 or 2) and differences in the size of both microspores (equal or not). Accessions TOM03 and Sorbo also showed signs of cytomixis (Supp. Figure S1).

To further test the sensitivity of male meiosis in Mt-0 to temperature, flowering plants were subjected to 4°C, 28°C and 32°C for different durations (Figure 2g). After 48h at 28°C, Mt-0 produced 1.8% dyads (n=764), a minor fraction of triads and otherwise normal tetrads (Figure 2h), indicating that male meiosis in Mt-0 is quite robust. Considering that male meiosis in Col-0 takes 26 hours from leptotene to tetrad microspore stage (Prusicki et al. 2019), a 24h heat treatment followed by immediate visualisation should reveal defects that

originate from any of the meiotic substages (Figure 2g). The exposure of Mt-0 to 32°C for 12h resulted in 100% normal tetrads (n=538) when analysed immediately after the treatment, indicating that high temperature did not affect cytokinesis or cell wall formation directly, but that dyad formation was likely the result of defects taking place during or right after meiosis I. Assuming that the duration of Mt-0 male meiosis is similar to that of Col-0, and that meiotic progression is generally accelerated at elevated temperature (De Jaeger-Braet et al. 2022), heat treated plants were allowed to recover for 6 and 12 hours before tetrad microspore analysis. A 6h recovery at 20°C after heat caused an increase in the frequency of dyads and triads to 59.4% and 2.1% respectively (n=848), and after another 6h of recovery (for a total of 12h) the frequency of dyads and triads dropped again to 9.9% and 0.7% respectively (n=288) (Figure 2h). Taken together, these results show that dyad formation in Mt-0 is not a direct consequence of increased temperature during meiosis II, but rather originates from a defect during earlier meiotic stages from zygotene to the onset of meiosis II.

Cold stress is also known to induce meiotic restitution in Arabidopsis (De Storme et al. 2012). In order to find a link with the high temperature induced dyad phenotype, accessions Mt-0, Copac-1 and Vimmerby were subjected to 4°C for 48h. Sampling on time points 0h, 24h and 48h after the treatment revealed no excessive defects at the tetrad-stage (Supp. Figure S2), indicating that the molecular mechanisms that causes these accessions to be heat sensitive at the tetrad-stage does not confer a hypersensitivity to cold.

Heat affects chromosome pairing in meiosis I and metaphase II progression in Mt-0

As indicated by the tetrad microspore analyses, Mt-0 follows the canonical progression through male meiosis under control conditions. Chromosomes condensate and synapse progressively during leptotene and zygotene to yield clearly distinguishable, fully synapsed threads at pachytene (Figure 3a). The synaptonemal complex degrades and the chiasmata between homologous chromosomes become visible in the 5 bivalents at diakinesis (Figure 3b). Subsequently the 5 bivalents align on the metaphase I plane (Figure 3c) and are separated during anaphase I (Figure 3d). Some of the homologous chromosomes are connected by chromosome strands but ultimately these are resolved to yield 2 equally divided chromosome sets at interkinesis (Figure 3e). Next, chromosomes align on 2 perpendicular metaphase II planes (Figure 3f) and are separated into 4 equal sets during anaphase II (Figure 3g) to yield balanced tetrads of 4 haploid microspores (Figure 3h).

169

170 After 32°C heat treatment for 24h, pachytene stage chromosomes appeared more loosely
171 arranged and showed partial synapsis in 57% of the meiocytes (n=98; Figures 3i, q).
172 Following the defects at pachytene, univalent chromosomes were observed at diakinesis and
173 metaphase I (19% and 19% as n=43 and 67 respectively; Figures 3j, k), indicating for the
174 partial loss of obligate crossover formation during previous stages. At diakinesis,
175 chromosome bridges between non-homologous chromosomes were observed which did not
176 occur at the control temperature (35%, n=43; Figure 3r). At anaphase I, chromosome bridges
177 and lagging chromosomes were observed more frequently (71%, n=21; Figures 3l, t). These
178 combined defects resulted occasionally in unbalanced sets of chromosomes or restituted
179 meiocytes at interkinesis (12.5%, n=40; Figure 3u), but mostly balanced sets of 5
180 chromosomes separated by a clear organelle band were observed (Figure 3m).

181

182 Meiosis progressed with the second meiotic division in heat treated plants with the formation
183 of perpendicular metaphase II plates (n=19; Figures 3n, v). In contrast to meiosis in control
184 plants, the separation of the chromatids during anaphase II towards the poles was never
185 observed in any of the plants analysed (n=9). Instead, we observed partial or no segregation
186 of the sister chromatids in meiocytes at anaphase II (n=13; Figures 3o, w). At the end of
187 telophase II, the chromosomes decondensed and formed dyads (57%, n=88; Figure 3p), triads
188 (16%; Figure 3x) and tetrads (27%). Altogether, these observations suggest that heat stress
189 causes an arrest of metaphase II progression.

190

191 **High dyads after heat phenotype maps to TAM**

192

193 An outcross analysis between ecotypes Mt-0 and Ler showed that the heat stress induced high
194 dyad phenotype of Mt-0 is linked with a single recessive locus (Supp. Figure S3a and Supp.
195 Table S4). Subsequent bulked segregant analysis mapped the locus to a 2.4Mbp region on the
196 bottom of chromosome 1 (Supp. Figure S3b). A prime candidate in this region with known
197 function in progression through the second meiotic division is TAM. A recessive, heat
198 sensitive EMS mutation (tam-1) was previously reported by Magnard et al. (2001) and Wang
199 et al. (2004). To check whether the heat sensitive Mt-0 locus corresponds to TAM, a
200 complementation test was performed by crossing Mt-0 with wild type Col-0 and the tam-1
201 mutant (in Col-0 background). Under control conditions (20°C) tam-1 produces a small
202 amount of dyads and triads, but this shifts to nearly 100% dyads after a 24h at 32°C heat

203 treatment, whereas Col-0 still produces mainly tetrads after this treatment (Supp. Figure S3c;
204 similarly to what was reported by Magnard et al. (2001) and De Storme and Geelen (2020)).
205 The Col-0 TAM allele complemented the Mt-0 heat induced high dyad phenotype, whereas a
206 Mt-0 tam-1 heterozygous F1 still displayed heat induced dyad formation (Supp. Figure S3c).
207
208 Subsequently Mt-0 and Ler were used as tester lines to complement the most heat sensitive
209 accessions revealed in our initial tetrad-stage screen. Several F1 lines were generated, and
210 tetrad-stage microspores were analysed after a 24h at 32°C treatment. For 7 accessions it was
211 found that they were unable to complement the heat induced dyad phenotype of Mt-0,
212 whereas in crosses with Ler, the dyad phenotype was suppressed (Figure 4). These results
213 identify TAM as the heat sensitive allele leading to dyad formation in at least 8 natural
214 accessions of Arabidopsis thaliana.
215
216 **High temperature stimulates TAM expression**
217
218 To elucidate how genomic sequence variation could lead to variation in the sensitivity for
219 heat induced meiotic restitution in natural Arabidopsis populations, we checked the SNP
220 frequency across the TAM locus using the available polymorphisms data of 1135 Arabidopsis
221 accessions (Alonso-Blanco et al. 2016; Figure 5a). As expected by natural selection pressure
222 and mutation bias (Monroe et al. 2022), SNP frequencies appeared higher in the 3'UTR and
223 5'UTR exons and the upstream region compared to the gene body. Notably, the occurrence of
224 non-synonymous SNPs appeared very low in the conserved N-terminal cyclin domain,
225 indicative for this domain to be essential for TAM functionality (Jeffrey et al. 1995; Wang et
226 al. 2004). Next, this dataset was used to compare the rarity of SNPs between the 8 TAM
227 sensitive accessions and 10 of the least sensitive accessions in our screen (in addition to Ler
228 and the Col-0 reference; Supp. Files 2 and 3). Indeed, we found that 5/8 of the sensitive lines
229 carried 1 or more rare SNPs (i.e., 50/1135 or less accessions share a SNP at this location)
230 compared to only 3/12 for the non-sensitive lines. Most of these rare SNPs were in the
231 5'UTR or further upstream, suggesting for effects on TAM expression. A notable exception
232 is the occurrence of a unique SNP leading to a missense variant in the conserved N-terminal
233 cyclin domain of accession Nok-3.
234
235 Comparison of the relative TAM expression levels in flowerbuds of plants grown at 20°C or
236 after 24h at 32°C points towards an increase of TAM expression under high temperatures in 6

237 of the accessions analysed (Mt-0, Vimmerby, Nok-3, Etna-2, Tac-0 and Zdr-1), that is not
238 occurring in the Col-0 or tam-1 lines (Figure 5b). Overexpression of TAM by an exogenous
239 promotor was previously shown to induce dyad formation (Wang and Yang 2014),
240 suggesting that increased levels of TAM transcription upon heat stress is part of the
241 mechanism leading to dyad formation. To confirm the role of TAM expression regulation in
242 heat induced dyad formation and to differentiate between the role of the 5'UTR and any
243 upstream regulatory sequences, 25 chimeric constructs were created combining the TAM
244 RNA coding genomic region with the upstream regions of 5 natural accessions (Figure 5c).
245 These constructs were terminated with a C-terminal GFP tag and transformed to the heat
246 sensitive tam-1 mutant background. The resulting T1 lines were analysed after a 24h at 32°C
247 heat treatment for dyad formation (Figure 5d). To minimize the impact of T-DNA insertion
248 position and genomic background effects, 5 T1 lines per construct were analysed. Hence why
249 the minimal average dyad production frequency of the constructs was around 25% and
250 maximally around 75% (Figure 5d). ANOVA analysis shows a statistically significant impact
251 of the upstream region on the average dyad production ($p=0.01$), but not for the RNA region
252 ($p=0.06$). Post-hoc pairwise comparisons show a significant difference between the Ler and
253 the Mt-0 or Tac-0 upstream region ($p=0.02$ and $p=0.03$, respectively) and nearly between the
254 Ler and Vimmerby or Nok-3 upstream region ($p=0.06$ and $p=0.11$, respectively). Although
255 not statistically significant, the Nok-3 RNA region appears to increase the heat sensitivity
256 ($p=0.08$ for the comparison between Nok-3 and Ler or Vimmerby), in accordance with this
257 natural accession carrying a unique missense SNP in the conserved N-terminal cyclin
258 domain. From these results we infer that mainly the upstream region has the potential to
259 confer the heat induced dyad phenotype with possibly Nok-3 showing a contribution also
260 from the RNA region.
261
262 **DNA methylation is not likely responsible for regulating TAM expression under heat**
263
264 High temperatures are known to modify DNA methylation patterns and plant development
265 (Naydenov et al. 2015; Chen et al. 2016; Kawakatsu et al. 2016; Malik 2022). Data from the
266 1001 epigenomes project (Kawakatsu et al. 2016) revealed that the TAM promotor contains
267 very few DNA methylation marks in leaf material of most accessions at control temperature
268 conditions (Supp. Figure S4). Therefore, we hypothesised that DNA methylation might
269 suppress TAM expression in Col-0 flowerbuds under heat, but not in Mt-0 due to the
270 presence of CG, CHG or CHH (H is A, T or C) site altering SNPs in the promotor region.

271

272 To check the methylation pattern of TAM we used bisulfite converted DNA extracted from
273 flowerbuds of Col-0 and Mt-0 grown at 20°C or heat treated for 24h at 32°C and compared
274 the methylation status of cytosine residues that were affected by a SNP in the Mt-0 TAM
275 promotor region (Table 1). This revealed no differences in the methylation status of the Col-0
276 promotor under both temperatures and no differential methylation between the Col-0 and the
277 Mt-0 promotor. In the absence of differential methylation of the TAM promotor under high
278 temperatures, it is unlikely that heat induced TAM expression and the associated dyad
279 phenotype is mediated by altered DNA methylation.

280

281 **Short term heat treatment induces enlarged pollen**

282

283 To investigate the impact of these heat induced meiotic defects on further pollen
284 development, pollen size of Mt-0 was monitored for 10 days after a 24h at 32°C heat
285 treatment using a Coulter Counter (De Storme et al. 2013). Pollen were collected from
286 individual, freshly opened flowers along the main inflorescence on the morning of every new
287 day (Figure 6a) and compared to a control that was kept at 20°C.

288

289 Under control conditions Mt-0 pollen samples form a Gaussian particle size distribution of
290 which 90% of the particles consistently measure between 16µm-23µm (Figure 6b, d). We
291 consider this to be normal-sized pollen. Smaller fractions consist of small particles (10µm-
292 16µm; about 7%) and large particles (23µm-30µm; about 3%) which we consider to be
293 mainly a mixture of dust and plant debris. After a 24h at 32°C heat treatment pollen quality
294 was decreased compared to the control as indicated by an increase of small particles across 2-
295 9 dpt (Figure 6c). On 3-4 dpt Alexander staining revealed the occurrence of shrivelled anthers
296 filled with dead pollen (58 out of 107 anthers; Figure 6j), suggesting for a somatic defect
297 harming all pollen in an anther during late pollen development. Contrary on 7-9 dpt anthers
298 appear swollen and contain a mixture of healthy purple pollen and shrivelled green coloured
299 cell (Figure 6k). This suggests a defect on the single meiocyte/microspore level, of which the
300 timing aligns with microspores receiving the heat treatment around the meiotic stage. Also,
301 on 8-9 dpt the fraction of large particles strongly increases to an average of about 20% across
302 all flowers analysed (Figure 6c). These large particles form a Gaussian peak around 25µm
303 that is clearly separated from the normal-sized pollen (Figure 6e). DAPI staining of these
304 samples reveals the presence of enlarged pollen grains with 1 enlarged vegetative and 2

305 enlarged sperm nuclei compared to the control (Figures 6f-i). On 10 dpt pollen size was
306 normal (Figure 6c) and viability fully recovered (Figure 6l), denoting the transient character
307 of the effects of short term heat treatment.
308
309 Particle size analysis was also used to investigate other high dyad producing accessions
310 (Supp. Figures S5 and S6). Under control conditions (20°C) most accessions show a
311 Gaussian particle size distribution with a single peak around 20µm (Supp. Figure S6),
312 exceptions are Etna-2, Sorbo, and Nok-3. These accessions consistently show next to a large
313 peak at 20µm, respectively a small peak of enlarged particles around 25µm, a small peak of
314 smaller particles around 18µm and a broad range of smaller particle between 10µm-20µm.
315 The latter group of small particles are likely empty pollen hulls generated by a heavy thrips
316 infection on the Nok-3 plants. The occurence of enlarged pollen in Etna-2 can be explained
317 by this accession's high stature phenotype bringing its flowerbuds close to the heat emitting
318 halogen lamps used in our growth rooms. This likely invokes diploid pollen production
319 through meiotic restitution, in accordance with this accession's high dyad phenotype after
320 heat. High temperatures (24h at 32°C) induced enlarged particles (>23µm) in most of these
321 accessions on 8-10dpt (Supp. Figure S5). Exceptions are Nok-3, for which particle
322 distributions do not differ remarkably from control conditions on these days, and Etna-2 that
323 shows a nearly complete loss of detectable particles between 7-10dpt. In addition to a peak at
324 25µm some accessions showed a shift to even larger pollen sizes (30µm), suggesting the
325 presence of higher level ploidy pollen (2n-4n; (De Storme et al. 2013)). From 10-11dpt pollen
326 particle size distributions were similar to the 20°C control in all accessions, in accordance
327 with the temporal impact of heat stress on pollen development (Supp. Figure S5).
328
329 **Heat induced sexual polyploidisation through 2n pollen**
330
331 Following our observations on the level of male meiosis and the known relationship between
332 pollen ploidy and size (De Storme et al. (2013) and references therein) we assumed that the
333 enlarged pollen of around 25µm after heat treatment never completed the second meiotic
334 division, but nevertheless continued through microspore development to form mature pollen
335 with a diploid (2n) chromosome number. To test this hypothesis, we used heat treated flowers
336 of Mt-0 of 7-9 dpt as both male and female parents in a reciprocal manual cross with Mt-0
337 kept at 20°C as well as allowed heat treated plants to self. Afterwards the resulting
338 offspring's ploidy was checked using flow cytometry. When heat treated Mt-0 was allowed to

339 self or used as the male parent we were able to detect triploid (3n) offspring on 8-9 dpt,
340 consistent with the appearance of enlarged pollen on those days (Table 2). No triploids could
341 be detected in a cross with heat treated Mt-0 as the female parent. Nine out of a total of 27
342 allegedly triploid plants were confirmed to be triploid (and not aneuploid) by counting the
343 number of chromosomes on mitotic chromosome spreads (Figure 7), indicating the viable 2n
344 pollen after heat treating Mt-0 likely results from a clean omission of the second meiotic
345 division.
346
347 **DISCUSSION**
348
349 Temperature stress leads to a variety of developmental defects in meiosis and microspore
350 development that have been extensively described across different organisms and kingdoms.
351 These defects typically include alterations or abolishment of cross over formation, meiotic
352 restitution and fertility defects (Zinn et al. 2010; Giorno et al. 2013; De Storme and Geelen
353 2014; Morgan et al. 2017; Rieu et al. 2017; Lloyd et al. 2018; Chaturvedi et al. 2021). It is
354 only recently that the genetic basis of these heat induced defects is being elucidated in plants.
355 Examples include the sporophitically expressed unfolded protein response component IRE1
356 (Deng et al. 2016), MAGO1 and MAGO2 that function in meiocyte initials in a transposon
357 surveillance mechanism (Lee et al. 2021) or the role of HSP101 in proper loading of RAD51
358 (Li et al. 2022). By exploiting the natural variation in Arabidopsis we here uncovered TAM
359 as a major molecular player in heat induced meiotic restitution.
360
361 **TAM functions in heat induced meiotic restitution**
362
363 Heat stress during meiosis is often associated with defects in microtubule (MT) organisation,
364 leading to parallel or fused spindles during metaphase or issues with RMA biogenesis
365 resulting in faulty chromosome separation, cytokinesis and meiotic restitution (Pécrix et al.
366 2011; Wang et al. 2017; De Storme and Geelen 2020). Although best characterised for its
367 role in meiotic progression (Magnard et al. 2001; Bulankova et al. 2010; Cifuentes et al.
368 2016) recent work has shown the involvement of TAM in MT organisation during meiosis
369 (Prusicki et al. 2019). Both functions are likely driven by modulation of CDKA;1 activity at
370 the level of individual meiocytes in a quantitative manner (Prusicki et al. 2019; Sofroni et al.
371 2020). Indeed, altered CDKA;1 activity levels cause defects in cytokinesis and MT
372 organisation similar to those observed in tam mutants (Sofroni et al. 2020). Although it is not

373 clear from our study whether the TAM-based heat induced meiotic restitution phenotype is
374 due to defects in MT organisation or meiotic progression (or both), the histological and
375 developmental differences of microspores between the different heat sensitive accessions and
376 the variable cell fates for meiocytes (dyad, triad, tetrad) within an accession reveal a
377 quantitative heat sensitivity phenotype. As a prime example of this stochastic, quantitative
378 process is the discrepancy between the number of heat induced dyads and the number of
379 unreduced mature pollen in all accessions, that cannot be accounted for by pollen death. This
380 is suggestive for the idea that a portion of the heat induced dyads continue their meiotic
381 development into haploid microspores in accordance with the previously reported
382 asynchronous meiotic phenotype of TAM (Magnard et al. 2001; Wang et al. 2004) and
383 successive cytokinesis in CDKA;1 reduced activity mutants (Sofroni et al. 2020; Yang et al.
384 2020). Further studies can help to dissect the quantitative nature of this phenotype and/or
385 reveal other molecular mechanisms that determine it.
386
387 **The influence of TAM expression on CDK activity**
388
389 Rather than a loss of or reduced TAM function, our data show that TAM expression is
390 increased after 24h at 32°C compared to a 20°C control in several high dyad producing
391 accessions, but not in the less sensitive Col-0 background. Remarkably Ning et al. (2021)
392 report an increase in TAM expression in Col-0 when temperatures are increased to 36°C and
393 there are indications that a high temperature induced reduction of TAM expression lead to
394 meiotic restitution in poplar (Zhou et al. 2022).
395
396 These contrasting observations raise the question as to how both TAM loss-of-function and
397 TAM overexpression (OE) can lead to meiotic restitution. Wang and Yang (2014) addressed
398 this by ectopic expression of TAM through the ASK1 promotor and discovered that both
399 TAM loss-of-function and OE mutants influence the dynamics of structural chromosome axis
400 protein ASY1, albeit each in a different manner. However, a 32°C heat treatment does not
401 influence ASY1 localisation nor TAM expression in Col-0 (De Storme and Geelen (2020)
402 and this study), whereas at 36°C both of these factors are affected (Ning et al. 2021). The
403 correct loading of ASY1 as well as ectopic meiotic cytokinesis and restitution are linked with
404 CDKA;1 activity (Wijnker et al. 2019; Sofroni et al. 2020; Yang et al. 2020). Because
405 phosphorylation by CDKA;1 of e.g. ASY1 (Yang et al. 2020) and TDM1 (Cifuentes et al.
406 2016) requires the interaction with TAM, we propose that this three-way protein interaction is

407 subject to a stoichiometric balance determining CDKA;1 activity. In the absence of TAM,
408 CDKA;1 loses partly the capacity to phosphorylate, leading to defects in chromosome axis
409 formation due to lack of ASY1 phosphorylation, and an early exit after MI through lack of
410 TDM1 phosphorylation. The quantitative nature of these defects is stipulated by the gradation
411 of severity of both phenotypes observed in the hypomorphic mutant tam-1 and the full KO
412 mutant tam-2 (Wang et al. 2004; d'Erfurth et al. 2010; Wang and Yang 2014)). When TAM
413 is overexpressed (TAM OE), CDKA;1 and/or its substrates are titrated away causing a
414 stoichiometric imbalance (Prelich 2012; Wang et al. 2014), leading to defects similar as in a
415 TAM loss-of-function mutant. Consequently, TAM expression levels in the single meiocytes
416 determines whether meiotic restitution happens or not. This can explain why we observed no
417 direct link between the relative amount of TAM OE after heat and the number of dyads
418 produced after heat. Similarly it can explain why the Mt-0 high dyad phenotype appears
419 recessive despite being based on TAM OE. The intermediate level of OE after heat in a
420 heterozygous background (Col-0/Mt-0 or Ler/Mt-0) is not sufficient to cause a CDKA;1
421 interaction imbalance and therefore dyad numbers are much lower than what is observed in
422 the wild type Mt-0.
423
424 CDKA;1 activity may also be affected by other factors under heat stress. Notably, heat stress
425 induces the formation of stress granules (Protter and Parker 2016). These are protein-mRNA
426 aggregates that steer the stress translatome and have been shown to contain CDKA;1 in
427 somatic and germline cells (Kosmacz et al. 2019; De Jaeger-Braet et al. 2022).
428
429 **Unreduced gametes, rare variants and plant evolution**
430
431 Unreduced gamete formation under changing environmental conditions has been proposed to
432 be an important driver of ancient and recent polyploidisation events which have a profound
433 impact on plant evolution (Bretagnolle and Thompson 1995; Vanneste et al. 2014; Novikova
434 et al. 2018; Fox et al. 2020; Van de Peer et al. 2021). We here show that heat stress not only
435 results in meiotic restitution and pollen death, but also lead to the production of viable 2n
436 pollen producing triploid offspring in Arabidopsis, as has been shown in other plant species
437 (Zhang et al. 2003; Lokker et al. 2005; Tian et al. 2018). Interestingly, we uncovered mainly
438 rare sequence variants of TAM in the highest dyad producing accessions, rather than a single
439 common variant. Since there are no indications that these variants disturb TAM's function
440 under normal temperature conditions, SNPs that confer heat sensitivity are tolerated in the

441 natural Arabidopsis population. Rare variants can have a major impact on complex
442 quantitative traits (e.g. in humans (Wainschtein et al. 2022), and yeast (Bloom et al. 2019))
443 and have the potential to play an important role in adaptation to changing environmental
444 conditions (e.g. in sea urchin (Brennan et al. 2019)). Rare allelic variants of TAM may hence
445 have contributed to the many plant whole genome duplication observed in plants. By
446 extension it should be noted that cyclin-CDK complexes regulate cell cycles both in
447 reproductive and somatic tissues (Wijnker and Schnittger 2013; Qi and Zhang 2020). As both
448 tissue types are subject to genome duplication under stressful conditions (Fox et al. 2020), we
449 anticipate that it will be interesting to investigate allelic variation of cyclins controlling
450 somatic cell divisions under various stress conditions.
451
452 **MATERIAL AND METHODS**
453
454 **Plant material and growth conditions**
455
456 For the initial tetrad-stage screen, 212 natural Arabidopsis accessions were selected (Lardon
457 et al. (2020). The tam-1 mutant (Wang et al. 2004) was kindly provided by Ming Yang
458 (Oklahoma State University). Genotyping primers are shown in Supp. Table S5.
459
460 Seeds were sterilized using chlorine gas and sown on growth medium (for 1l of medium:
461 2.154g MS without vitamins, 10g sucrose, 100mg myo-inositol and 0.5g MES, 8g agar. pH
462 adjusted to 5.7. 50mg kanamycin was added for antibiotic selection). Seeds were vernalised
463 for 3 days at 4°C in the dark and moved to 21°C and 16h/8h light/dark for germination. After
464 5 days, seedlings were transferred to soil substrate (Jiffy) and grown at 20°C under 12h/12h
465 light/dark for 3-4 weeks with regular watering supplemented with liquid fertilizer (Wuxal).
466 Afterwards, plants were grown at 20°C and 16h/8h light/dark without fertilizer to stimulate
467 flowering. Relative humidity was kept at 60%-70%. For experiments after the initial tetrad-
468 stage screen, a 10 week cold treatment at 4°C and 16h/8h light/dark was used for accessions
469 Vimmerby, Nok-3, Tac-0, Ta-0, Etna-2, TOM03, Sorbo, Or-1, Tha-1, before moving them to
470 20°C to stimulate even flowering.
471
472 For temperature experiments, healthy looking, flowering plants with at least 3 siliques on the
473 main inflorescence axis were transferred to a Panasonic MLR-352H-PE versatile

environmental test chamber under similar growing conditions, but with different temperatures (4°C, 28°C, 32°C) for the duration of the treatment (12h, 24h, 48h).

Tetrad-stage analysis

Accessions were divided into 54 batches (G1-G54) based on their flowering time under 16h/8h light/dark. Three plants for every accession were kept at 20°C and 10 plants were heat treated for 24h at 32°C. Immediately after the treatment, tetrad-stage flowerbuds of the main inflorescence were dissected and stained with lactopropionic orcein (De Storme and Geelen (2020). For every individual plant the number of tetrad-, triad- and dyad-configurations was recorded. Accessions with at least 3 individual heat treated plants with at least 20 tetrad-stage configuration counts were selected for further analysis. The number of tetrads, triads and dyads were converted to a percentage for every plant and the mean value and standard error were calculated for every accession and treatment. A Kruskal-Wallis rank-sum test on the mean dyad production revealed no batch effect ($p=0.32$).

Aniline blue staining of tetrad-stage microspores to stain the callose walls was done according to Johnson-Brousseau and McCormick (2004).

Male meiotic chromosome spreads

DAPI staining of enzyme digested chromosome spreads of male meiotic flowerbuds was done according to Ross et al. (1996) with modifications mentioned in De Storme and Geelen (2020). The same technique was used to observe somatic chromosome spreads.

F2 mapping analysis

The F2 generation of a cross between Ler and Mt-0 was heat treated (24h 32°C) during the flowering stage and individual plants were checked for high dyad production at the tetrad-stage. Leaf samples of the high dyad producing plants were stored at -80°C before DNA extraction with the Wizard genomic DNA purification kit (Promega). A pooled DNA sample

508 (equal mass) was sent for sequencing on an Illumina NextSeq500 PE150 platform for a total
509 of 36Gb output (predicted coverage: 60x). Adapter and low quality reads were removed with
510 Trimmomatic v0.39 using standard parameters (Bolger et al. 2014). Duplicate reads were
511 removed with FastUniq v1.1 (Xu et al. 2012) and quality was monitored using FastQC
512 v0.11.2 (Andrews et al. 2014). Aligning, mapping and annotation were performed with
513 SHOREmap v3.0, according to Sun and Schneeberger (2015).

514 **Analysis of SNP frequencies**

515

516 SNP and indel frequencies for the genomic positions of the TAM/CYCA1;2 locus (chr1:
517 29081654..29085477) were extracted from the 1001 genomes database
518 (https://tools.1001genomes.org/polymorph/ (Alonso-Blanco et al. 2016)), or our own
519 resequencing data in case of Mt-0. Positions of relevant genomic regions and functional
520 protein domains were extracted from EnsemblPlants (https://plants.ensembl.org/index.html).
521 Data were reformatted using custom made R scripts.

522

523 **Two-step RT-qPCR**

524

525 Immediately after the treatment (20°C or 24h at 32°C) all unopened flowerbuds on the main
526 axis were frozen in liquid N_2 before RNA extraction using the Promega ReliaPrep RNA
527 Tissue Miniprep System. RNA purity and quantity were checked with Nanodrop and 1µg of
528 total RNA was used as starting material for first strand cDNA synthesis using the Promega
529 GoScript Reverse Transcription System with oligo(dT) primers. Two µl of cDNA (1:4
530 dilution) was added to a 20µl qPCR reaction using the GoTaq qPCR Master Mix (Promega)
531 and ran on a BioRad CFX Opus96 thermocycler. Cycles were as follows: 2min at 95°C, 40x
532 (15s at 95°C and 40s at 60°C). Quality was checked by melting curve analysis and gel
533 electrophoresis of the PCR products. For each accession 3 individual plants were used per
534 treatment (biological replicates) and 3 technical replicates were performed per sample. Data
535 were analysed using the ΔΔCt method as described in Taylor et al. (2019) using the R pcr
536 package (Ahmed and Kim 2018), with EF1αA4 as the reference gene (Ning et al. 2021), and
537 normalized to the 20°C control for each accession. Primers are shown in Supp. Table S5.

538

539 **Plasmid construction and transformation**

540

541 Chimeric constructs of TAM/CYCA1;2 upstream and RNA genomic regions were cloned
542 using the Multisite-Gateway cloning system (Invitrogen). Primers for cloning the
543 TAM/CYCA1;2 upstream and RNA genomic regions are given in Supp. Table S5. All 25
544 combinations of upstream and RNA genomic regions were coupled to a C-terminal GFP
545 moiety in a three way gateway reaction. Plasmids were checked through enzyme digestion
546 and sequencing before moving them to Agrobacterium tumefaciens strain GV3130. Floral dip
547 was used to transform tam-1 plants. Transformed plants were selected based on kanamycin
548 resistance.
549
550 **DNA methylation analysis**
551
552 DNA was extracted from Mt-0 and Col-0 flowerbuds grown at 20°C and 24h 32°C, in 3
553 biological replicates. DNA was extracted with the Wizard genomic DNA purification kit
554 (Promega) and bisulfite converted with the ThermoFisher epiJET bisulfite conversion kit.
555 Next, regions were amplified by PCR using primers designed with the ZYMO free bisulfite
556 primer design tool (https://www.zymoresearch.com/pages/bisulfite-primer-seeker). Primers
557 are listed in Supp. Table S5. Successful amplicons were Sanger sequenced.
558
559 **Pollen particle size analysis**
560
561 A single, freshly opened flower was picked from the main inflorescence and placed in 1ml of
562 Isoton II solution. After vortexing to release the pollen and removal of the flower material the
563 solution was diluted in 10ml of Isoton II and measured using a Beckman Mulitisizer II
564 Coulter counter as previously described (De Storme et al. 2013). For each treatment 3 or 4
565 individual plants were used that produced 1-3 open flowers on the main inflorescence per
566 day. Analysis based on size thresholds was done using a custom R script. Samples with less
567 than 200 particle counts were removed from the particle size analysis.
568
569 **Alexander staining of mature pollen**
570
571 After dissecting the anthers from nearly opened flowers (before anther dehiscence), viability
572 staining was performed as described by Alexander (1969).
573
574 **DAPI staining of mature pollen**

575

576 To visualise the nuclei in mature pollen grains open flowers were placed in 200µl of citrate-
577 phosphate buffer at pH 4, with 1% triton X-100 and 1µg/ml DAPI (Vergne et al. 1987). After
578 vortexing and removal of the flower material samples were incubated for 20min in the dark.
579 The solution was centrifuged to pellet the pollen and the pellet was resuspended in 20µl of
580 staining solution before visualisation.

581 **Plant ploidy analysis**

582

583 Somatic ploidy determination was done based on the nuclear extraction method described by
584 Galbraith et al. (1983) on fresh leaf material as described by De Storme and Geelen (2011).
585 Stained samples were analysed on a BD FACSVerse flow cytometer.

586

587 **Microscopy**

588

589 Microscopic images were taken using an Olympus IX81 microscope with an X-Cite 120 LED
590 boost lamp equipped with an Olympus XM10 camera and Olympus Cell M software. Images
591 after Alexander staining were taken on an Olympus BX51 with a ColorView III camera and
592 Cell F software.

593

594 **Statistical analyses**

595

596 Statistical analyses and methods are defined in the relevant figure or table captions and the
597 relevant text sections.

598

599 **Supplemental Data**

600

601 **Supplemental Figure S1** High dyad after heat accessions' tetrad stage phenotype.
602 **Supplemental Figure S2** The influence of cold on high dyads after heat producing
603 accessions.
604 **Supplemental Figure S3** Mapping of the Mt-0 locus.
605 **Supplemental Figure S4** Methylation pattern of the TAM/CYCA1;2 promotor.
606 **Supplemental Figure S5** Pollen particle size time series for 8 high dyad after heat producing
607 accessions.

608 **Supplemental Figure S6** Pollen particle size distribution for 8 high dyad after heat
609 producing accessions.
610 **Supplemental Table S1** Quantification of callose wall phenotypes for multiple accessions.
611 **Supplemental Table S2** Quantifications of nuclei per cell at the tetrad stage for multiple
612 accessions.
613 **Supplemental Table S3** Quantification of balanced and unbalanced meiocytes at the tetrad
614 stage for multiple accessions.
615 **Supplemental Table S4** Analysis of the segregation pattern of the Mt-0 locus.
616 **Supplemental Table S5** Primers used in this study.
617
618 **Supplemental File 1** Information on the 172 accessions retained for analysis in the tetrad-
619 stage screen after 24h at 32°C (HS).
620 Including geographical location (Lat and Long), treatment batch (G1-G54), the number of
621 plants analysed (n) and the mean frequency and standard deviation (SD) of dyad, triad and
622 tetrad production. Ranked according to mean dyad production.
623
624 **Supplemental File 2** Tabular overview of the SNPs of the TAM/CYCA1;2 locus for multiple
625 accessions.
626 Frequency of SNPs and indels at genomic positions of the TAM/CYCA1;2 locus (chr1:
627 29081654..29085477) for 8 high frequency, heat induced dyad producing accessions
628 (Vimmerby, Nok-3, Etna-2, Tac-0, Ta-0, Or-1, Tha-1, Mt-0) and for 12 of the lowest
629 frequency dyad producing accessions (Col-0, Ler-0, Litva, Zdr-1, Angit-1, RRS-7, Angel-1,
630 Di-G, Bsch-0, Uod-1, Gel-1, Tol-0). Ranked according to the rarity of the SNPs and indels.
631 Positions with a SNP/indel frequency <= 50 in any of the 8 high dyad producing accessions
632 are coloured yellow and information is added on the genomic location and the consequence
633 of the SNP/indel. SNP/indel data were obtained from
634 https://tools.1001genomes.org/polymorph/ (Alonso-Blanco et al. 2016) or our own
635 resequencing data in case of Mt-0.
636
637 **Supplemental File 3** Multiple sequence alignment of the TAM/CYCA1;2 genomic sequence.
638 Multiple sequence alignment of the TAM/CYCA1;2 genomic sequence (chr1:
639 29081654..29085477) for 8 high frequency, heat induced dyad producing accessions
640 (Vimmerby, Nok-3, Etna-2, Tac-0, Ta-0, Or-1, Tha-1, Mt-0) and for 12 of the lowest

641 frequency dyad producing accessions (Col-0, Ler-0, Litva, Zdr-1, Angit-1, RRS-7, Angel-1,
642 Di-G, Bsch-0, Uod-1, Gel-1, Tol-0).
643
644 **ACKNOWLEDGMENTS**
645
646 The authors would like to thank Ming Yang for providing the tam-1 seeds. Limin Sun, Robin
647 Lardon and Steffen Vanneste are thanked for the helpful discussions. We are grateful to
648 Christophe Petit, Ellen Van Gysegem and Patricia Delaere for technical support. This work
649 was supported by the Research Foundation—Flanders (FWO), through a Ph.D. fellowship to
650 Cédric Schindfessel (Grant No. 11G7421N) and Chunlian Jin was supported by a CSC grant
651 No. 201606350011.
652
653 **AUTHOR CONTRIBUTIONS**
654
655 CS and DG designed the experiments. CS and CJ performed the experiments. CS analysed
656 and visualised the data. CS and DG wrote the manuscript.
657
658 **COMPETING INTERESTS**
659
660 The authors declare no competing interests

661 **REFERENCES**

662

663 Ahmed M, Kim DR (2018) pcr: An R package for quality assessment, analysis and testing of
664 qPCR data. PeerJ 2018:. https://doi.org/10.7717/peerj.4473
665 Alexander MP (1969) Differential staining of aborted and nonaborted pollen. Stain
666 technology 44:117–122. https://doi.org/10.3109/10520296909063335
667 Alonso-Blanco C, Andrade J, Becker C, Bemm F, Bergelson J, Borgwardt KMM, Cao J,
668 Chae E, Dezwaan TMM, Ding W, Ecker JRR, Exposito-Alonso M, Farlow A, Fitz J,
669 Gan X, Grimm DGG, Hancock AMM, Henz SRR, Holm S, et al (2016) 1,135 Genomes
670 Reveal the Global Pattern of Polymorphism in Arabidopsis thaliana. Cell 166:481–491.
671 https://doi.org/10.1016/j.cell.2016.05.063
672 Andreuzza S, Nishal B, Singh A, Siddiqi I (2015) The Chromatin Protein DUET/MMD1
673 Controls Expression of the Meiotic Gene TDM1 during Male Meiosis in Arabidopsis.
674 PLoS Genetics 11:1–22. https://doi.org/10.1371/journal.pgen.1005396
675 Andrews S, Krueger F, Seegonds-Pichon A, Biggins L, Krueger C, Wingett S (2014) FastQC:
676 a quality control tool for high throughput sequence data. In: FastQC: a quality control
677 tool for high throughput sequence data.
678 http://www.bioinformatics.babraham.ac.uk/projects/fastqc. Accessed 5 Oct 2020
679 Bac-Molenaar JA, Fradin EF, Becker FFM, Rienstra JA, van der Schoot J, Vreugdenhil D,
680 Keurentjes JJB (2015) Genome-wide association mapping of fertility reduction upon
681 heat stress reveals developmental stage-specific QTLs in Arabidopsis Thaliana. Plant
682 Cell 27:1857–1874. https://doi.org/10.1105/tpc.15.00248
683 Bloom JS, Boocock J, Treusch S, Sadhu MJ, Day L, Oates-Barker H, Kruglyak L (2019)
684 Rare variants contribute disproportionately to quantitative trait variation in yeast. eLife
685 8:1–19. https://doi.org/10.7554/eLife.49212
686 Bolger AM, Lohse M, Usadel B (2014) Trimmomatic: A flexible trimmer for Illumina
687 sequence data. Bioinformatics 30:2114–2120.
688 https://doi.org/10.1093/bioinformatics/btu170
689 Bomblies K, Higgins JD, Yant L (2015) Meiosis evolves: Adaptation to external and internal
690 environments. New Phytologist 208:306–323. https://doi.org/10.1111/nph.13499
691 Brennan RS, Garrett AD, Huber KE, Hargarten H, Pespeni MH (2019) Rare genetic variation
692 and balanced polymorphisms are important for survival in global change conditions.
693 Proceedings of the Royal Society B: Biological Sciences 286:.
694 https://doi.org/10.1098/rspb.2019.0943

695 Bretagnolle F, Thompson JD (1995) Gametes with the somatic chromosome number:
696 mechanisms of their formation and role in the evolution of autopolyploid plants. New
697 Phytologist 129:1–22. https://doi.org/10.1111/j.1469-8137.1995.tb03005.x
698 Brownfield L, Köhler C (2011) Unreduced gamete formation in plants: Mechanisms and
699 prospects. Journal of Experimental Botany 62:1659–1668.
700 https://doi.org/10.1093/jxb/erq371
701 Brownfield L, Yi J, Jiang H, Minina EA, Twell D, Köhler C (2015) Organelles maintain
702 spindle position in plant meiosis. Nature Communications 6:.
703 https://doi.org/10.1038/ncomms7492
704 Bulankova P, Riehs-Kearnan N, Nowack MK, Schnittger A, Riha K (2010) Meiotic
705 progression in Arabidopsis is governed by complex regulatory interactions between
706 SMG7, TDM1, and the meiosis I-specific cyclin TAM. Plant Cell 22:3791–3803.
707 https://doi.org/10.1105/tpc.110.078378
708 Chaturvedi P, Wiese AJ, Ghatak A, Záveská Drábková L, Weckwerth W, Honys D (2021)
709 Heat stress response mechanisms in pollen development. New Phytologist 231:571–585.
710 https://doi.org/10.1111/nph.17380
711 Chen Y, Müller F, Rieu I, Winter P (2016) Epigenetic events in plant male germ cell heat
712 stress responses. Plant Reproduction 29:21–29. https://doi.org/10.1007/s00497-015-
713 0271-5
714 Cifuentes M, Jolivet S, Cromer L, Harashima H, Bulankova P, Renne C, Crismani W,
715 Nomura Y, Nakagami H, Sugimoto K, Schnittger A, Riha K, Mercier R (2016) TDM1
716 Regulation Determines the Number of Meiotic Divisions. PLoS Genetics 12:1–22.
717 https://doi.org/10.1371/journal.pgen.1005856
718 Cromer L, Heyman J, Touati S, Harashima H, Araou E, Girard C, Horlow C, Wassmann K,
719 Schnittger A, de Veylder L, Mercier R (2012) OSD1 promotes meiotic progression via
720 APC/C inhibition and forms a regulatory network with TDM and CYCA1;2/TAM.
721 PLoS Genetics 8:. https://doi.org/10.1371/journal.pgen.1002865
722 d'Erfurth I, Cromer L, Jolivet S, Girard C, Horlow C, Sun Y, To JPC, Berchowitz LE,
723 Copenhaver GP, Mercier R (2010) The CYCLIN-A CYCA1;2/TAM is required for the
724 meiosis I to meiosis II transition and cooperates with OSD1 for the prophase to first
725 meiotic division transition. PLoS Genetics 6:1–12.
726 https://doi.org/10.1371/journal.pgen.1000989
727 d'Erfurth I, Jolivet S, Froger N, Catrice O, Novatchkova M, Mercier R (2009) Turning
728 meiosis into mitosis. PLoS Biology 7:. https://doi.org/10.1371/journal.pbio.1000124

729 d'Erfurth I, Jolivet S, Froger N, Catrice O, Novatchkova M, Simon M, Jenczewski E, Mercier
730 R (2008) Mutations in AtPS1 (Arabidopsis thaliana Parallel Spindle 1) lead to the
731 production of diploid pollen grains. PLoS Genetics 4:1–9.
732 https://doi.org/10.1371/journal.pgen.1000274
733 De Jaeger-Braet J, Krause L, Buchholz A, Schnittger A (2022) Heat stress reveals a
734 specialized variant of the pachytene checkpoint in meiosis of Arabidopsis thaliana . The
735 Plant Cell 34:433–454. https://doi.org/10.1093/plcell/koab257
736 De Storme N, Copenhaver GP, Geelen D (2012) Production of diploid male gametes in
737 Arabidopsis by cold-induced Destabilization of postmeiotic radial microtubule arrays.
738 Plant Physiology 160:1808–1826. https://doi.org/10.1104/pp.112.208611
739 De Storme N, Geelen D (2014) The impact of environmental stress on male reproductive
740 development in plants: Biological processes and molecular mechanisms. Plant, Cell and
741 Environment 37:1–18. https://doi.org/10.1111/pce.12142
742 De Storme N, Geelen D (2013) Cytokinesis in plant male meiosis. Plant Signaling and
743 Behavior 8:. https://doi.org/10.4161/psb.23394
744 De Storme N, Geelen D (2020) High temperatures alter cross-over distribution and induce
745 male meiotic restitution in Arabidopsis thaliana. Communications Biology 3:1–15.
746 https://doi.org/10.1038/s42003-020-0897-1
747 De Storme N, Geelen D (2011) The arabidopsis mutant jason produces unreduced first
748 division restitution male gametes through a parallel/ fused spindle mechanism in meiosis
749 II. Plant Physiology 155:1403–1415. https://doi.org/10.1104/pp.110.170415
750 De Storme N, Zamariola L, Mau M, Sharbel TF, Geelen D (2013) Volume-based pollen size
751 analysis: An advanced method to assess somatic and gametophytic ploidy in flowering
752 plants. Plant Reproduction 26:65–81. https://doi.org/10.1007/s00497-012-0209-0
753 Deng Y, Srivastava R, Quilichini TD, Dong H, Bao Y, Horner HT, Howell SH (2016) IRE1,
754 a component of the unfolded protein response signaling pathway, protects pollen
755 development in Arabidopsis from heat stress. Plant Journal 88:193–204.
756 https://doi.org/10.1111/tpj.13239
757 Fox DT, Soltis DE, Soltis PS, Ashman TL, Van de Peer Y (2020) Polyploidy: A Biological
758 Force From Cells to Ecosystems. Trends in Cell Biology 30:688–694.
759 https://doi.org/10.1016/j.tcb.2020.06.006
760 Galbraith DW, Harkins KR, Maddox JM, Ayres NM, Sharma DP, Firoozabady E (1983)
761 Rapid flow cytometric analysis of the cell cycle in intact plant tissues. Science
762 220:1049–1051. https://doi.org/10.1126/science.220.4601.1049

763 Giorno F, Wolters-Arts M, Mariani C, Rieu I (2013) Ensuring reproduction at high
764 temperatures: The heat stress response during anther and pollen development. Plants
765 2:489–506. https://doi.org/10.3390/plants2030489
766 Jeffrey PD, Russo AA, Polyak K, Gibbs E, Hurwitz J, Massagué J, Pavletich NP (1995)
767 Mechanism of CDK activation revealed by the structure of a cyclinA-CDK2 complex.
768 Nature 376:313–320
769 Johnson-Brousseau SA, McCormick S (2004) A compendium of methods useful for
770 characterizing Arabidopsis pollen mutants and gametophytically-expressed genes. Plant
771 Journal 39:761–775. https://doi.org/10.1111/j.1365-313X.2004.02147.x
772 Kawakatsu T, Huang S shan C, Jupe F, Sasaki E, Schmitz RJJ, Urich MAA, Castanon R,
773 Nery JRR, Barragan C, He Y, Chen H, Dubin M, Lee CR, Wang C, Bemm F, Becker C,
774 O'Neil R, O'Malley RCC, Quarless DXX, et al (2016) Epigenomic Diversity in a Global
775 Collection of Arabidopsis thaliana Accessions. Cell 166:492–505.
776 https://doi.org/10.1016/j.cell.2016.06.044
777 Kosmacz M, Gorka M, Schmidt S, Luzarowski M, Moreno JC, Szlachetko J, Leniak E,
778 Sokolowska EM, Sofroni K, Schnittger A, Skirycz A (2019) Protein and metabolite
779 composition of Arabidopsis stress granules. New Phytologist 222:1420–1433.
780 https://doi.org/10.1111/nph.15690
781 Lardon R, Wijnker E, Keurentjes J, Geelen D (2020) The genetic framework of shoot
782 regeneration in Arabidopsis comprises master regulators and conditional fine-tuning
783 factors. Communications Biology 3:1–13. https://doi.org/10.1038/s42003-020-01274-9
784 Lee YS, Maple R, Dürr J, Dawson A, Tamim S, del Genio C, Papareddy R, Luo A, Lamb JC,
785 Amantia S, Sylvester AW, Birchler JA, Meyers BC, Nodine MD, Rouster J, Gutierrez-
786 Marcos J (2021) A transposon surveillance mechanism that safeguards plant male
787 fertility during stress. Nature Plants 7:34–41. https://doi.org/10.1038/s41477-020-
788 00818-5
789 Li Y, Huang Y, Sun H, Wang T, Ru W, Pan L, Zhao X, Dong Z, Huang W, Jin W (2022)
790 Heat shock protein 101 contributes to the thermotolerance of male meiosis in maize. The
791 Plant Cell
792 Li Y, Shen Y, Cai C, Zhong C, Zhu L, Yuan M, Ren H (2010) The type II Arabidopsis
793 formin14 interacts with microtubules and microfilaments to regulate cell division. Plant
794 Cell 22:2710–2726. https://doi.org/10.1105/tpc.110.075507
795 Lloyd A, Morgan C, Franklin FCH, Bomblies K (2018) Plasticity of meiotic recombination
796 rates in response to temperature in arabidopsis. Genetics 208:1409–1420.

797 https://doi.org/10.1534/genetics.117.300588
798 Lokker AC, Barba-Gonzalez R, Lim KB, Ramanna MS, Van Tuyl JM (2005) Genotypic and
799 environmental variation in production of 2n-gametes of oriental x asiatic lily hybrids.
800 Acta Horticulturae 673:453–456. https://doi.org/10.17660/ActaHortic.2005.673.58
801 Magnard J, Yang M, Chen YS, Leary M, Mccormick S (2001) Required for the Normal Pace
802 and Synchrony of Cell Division during Male Meiosis 1. Society 127:1157–1166.
803 https://doi.org/10.1104/pp.010473.1
804 Malik S (2022) Epigenetic Regulation of Heat Stress in Plant Male Reproduction. Frontiers in
805 Plant Science 13:. https://doi.org/10.3389/fpls.2022.826473
806 Mercier R, Mézard C, Jenczewski E, Macaisne N, Grelon M (2015) The Molecular Biology
807 of Meiosis in Plants. Annual Review of Plant Biology 66:297–327.
808 https://doi.org/10.1146/annurev-arplant-050213-035923
809 Mittler R, Finka A, Goloubinoff P (2012) How do plants feel the heat? Trends in
810 Biochemical Sciences 37:118–125. https://doi.org/10.1016/j.tibs.2011.11.007
811 Modliszewski JL, Copenhaver GP (2017) Meiotic recombination gets stressed out: CO
812 frequency is plastic under pressure. Current Opinion in Plant Biology 36:95–102.
813 https://doi.org/10.1016/j.pbi.2016.11.019
814 Monroe JG, Srikant T, Carbonell-Bejerano P, Becker C, Lensink M, Exposito-Alonso M,
815 Klein M, Hildebrandt J, Neumann M, Kliebenstein D, Weng ML, Imbert E, Ågren J,
816 Rutter MT, Fenster CB, Weigel D (2022) Mutation bias reflects natural selection in
817 Arabidopsis thaliana. Nature 602:101–105. https://doi.org/10.1038/s41586-021-04269-6
818 Morgan CH, Zhang H, Bomblies K (2017) Are the effects of elevated temperature on meiotic
819 recombination and thermotolerance linked via the axis and synaptonemal complex?
820 Philosophical Transactions of the Royal Society B: Biological Sciences 372:.
821 https://doi.org/10.1098/rstb.2016.0470
822 Naydenov M, Baev V, Apostolova E, Gospodinova N, Sablok G, Gozmanova M, Yahubyan
823 G (2015) High-temperature effect on genes engaged in DNA methylation and affected
824 by DNA methylation in Arabidopsis. Plant Physiology and Biochemistry 87:102–108.
825 https://doi.org/10.1016/j.plaphy.2014.12.022
826 Ning Y, Liu Q, Wang C, Qin E, Wu Z, Wang M, Yang K, Elesawi IE, Chen C, Liu H, Qin R,
827 Liu B (2021) Heat stress interferes with formation of double-strand breaks and homolog
828 synapsis. Plant Physiology 185:1783–1797. https://doi.org/10.1093/plphys/kiab012
829 Novikova PY, Hohmann N, Van de Peer Y (2018) Polyploid Arabidopsis species originated
830 around recent glaciation maxima. Current Opinion in Plant Biology 42:8–15.

831 https://doi.org/10.1016/j.pbi.2018.01.005
832 Omidi M, Siahpoosh MR, Mamghani R, Modarresi M (2014) The influence of terminal heat
833 stress on meiosis abnormalities in pollen mother cells of wheat. Cytologia 79:49–58.
834 https://doi.org/10.1508/cytologia.79.49
835 Osman K, Higgins JD, Sanchez-Moran E, Armstrong SJ, Franklin FCH (2011) Pathways to
836 meiotic recombination in Arabidopsis thaliana. New Phytologist 190:523–544.
837 https://doi.org/10.1111/j.1469-8137.2011.03665.x
838 Pécrix Y, Rallo G, Folzer H, Cigna M, Gudin S, Le Bris M (2011) Polyploidization
839 mechanisms: Temperature environment can induce diploid gamete formation in Rosa sp.
840 Journal of Experimental Botany 62:3587–3597. https://doi.org/10.1093/jxb/err052
841 Prelich G (2012) Gene overexpression: Uses, mechanisms, and interpretation. Genetics
842 190:841–854. https://doi.org/10.1534/genetics.111.136911
843 Protter DSW, Parker R (2016) Principles and Properties of Stress Granules. Trends in Cell
844 Biology 26:668–679. https://doi.org/10.1016/j.tcb.2016.05.004
845 Prusicki MA, Keizer EM, Van Rosmalen RP, Komaki S, Seifert F, Müller K, Wijnker E,
846 Fleck C, Schnittger A (2019) Live cell imaging of meiosis in arabidopsis thaliana. eLife
847 8:1–31. https://doi.org/10.7554/eLife.42834
848 Qi F, Zhang F (2020) Cell Cycle Regulation in the Plant Response to Stress. Frontiers in
849 Plant Science 10:1–10. https://doi.org/10.3389/fpls.2019.01765
850 Rieu I, Twell D, Firon N (2017) Pollen development at high temperature: From acclimation
851 to collapse. Plant Physiology 173:1967–1976. https://doi.org/10.1104/pp.16.01644
852 Ross KJ, Fransz P, Jones GH (1996) A light microscopic atlas of meiosis in Arabidopsis
853 thaliana. Chromosome Research 4:507–516. https://doi.org/10.1007/BF02261778
854 Schindfessel C, Drozdowska Z, De Mooij L, Geelen D (2021) Loss of obligate crossovers,
855 defective cytokinesis and male sterility in barley caused by short-term heat stress. Plant
856 Reproduction 34:243–253. https://doi.org/10.1007/s00497-021-00415-2
857 Sofroni K, Takatsuka H, Yang C, Dissmeyer N, Komaki S, Hamamura Y, Böttger L, Umeda
858 M, Schnittger A (2020) CDKD-dependent activation of CDKA;1 controls microtubule
859 dynamics and cytokinesis during meiosis. Journal of Cell Biology 219:.
860 https://doi.org/10.1083/JCB.201907016
861 Sun H, Schneeberger K (2015) SHOREmap v3.0: Fast and Accurate Identifi cation of Causal
862 Mutations from Forward Genetic Screens. In: Alonso JM, Stepanova AN (eds) Plant
863 Functional Genomics: Methods and Protocols: Second Edition, 2nd editio. Springer,
864 New York, pp 381–395

865 Taylor SC, Nadeau K, Abbasi M, Lachance C, Nguyen M, Fenrich J (2019) The Ultimate
866 qPCR Experiment: Producing Publication Quality, Reproducible Data the First Time.
867 Trends in Biotechnology 37:761–774. https://doi.org/10.1016/j.tibtech.2018.12.002
868 Tian M, Zhang Y, Liu Y, Kang X, Zhang P (2018) High temperature exposure did not affect
869 induced 2n pollen viability in Populus. Plant Cell and Environment 41:1383–1393.
870 https://doi.org/10.1111/pce.13165
871 Van de Peer Y, Ashman TL, Soltis PS, Soltis DE (2021) Polyploidy: an evolutionary and
872 ecological force in stressful times. The Plant cell 33:11–26.
873 https://doi.org/10.1093/plcell/koaa015
874 Vanneste K, Baele G, Maere S, Van De Peer Y (2014) Analysis of 41 plant genomes supports
875 a wave of successful genome duplications in association with the Cretaceous-Paleogene
876 boundary. Genome Research 24:1334–1347. https://doi.org/10.1101/gr.168997.113
877 Vergne P, Delvallee I, Dumas C (1987) Rapid assessment of microspore and pollen
878 development stage in wheat and maize usind DAPI and membrane permeabilization.
879 Stain technology 62:299–304. https://doi.org/10.1016/0960-0760(93)90156-Q
880 Wainschtein P, Jain D, Zheng Z, Cupples LA, Shadyab AH, McKnight B, Shoemaker BM,
881 Mitchell BD, Psaty BM, Kooperberg C, Liu CT, Albert CM, Roden D, Chasman DI,
882 Darbar D, Lloyd-Jones DM, Arnett DK, Regan EA, Boerwinkle E, et al (2022)
883 Assessing the contribution of rare variants to complex trait heritability from whole-
884 genome sequence data. Nature genetics 54:263–273. https://doi.org/10.1038/s41588-
885 021-00997-7
886 Wang J, Li D, Shang F, Kang X (2017) High temperature-induced production of unreduced
887 pollen and its cytological effects in Populus. Scientific Reports 7:1–12.
888 https://doi.org/10.1038/s41598-017-05661-x
889 Wang P, Zhou Z, Hu A, Pontede Albuquerque C, Zhou Y, Hong L, Sierecki E, Ajiro M,
890 Kruhlak M, Harris C, Guan KL, Zheng ZM, Newton AC, Sun P, Zhou H, Fu XD (2014)
891 Both decreased and increased SRPK1 levels promote cancer by interfering with PHLPP-
892 mediated dephosphorylation of Akt. Molecular Cell 54:378–391.
893 https://doi.org/10.1016/j.molcel.2014.03.007
894 Wang Y, Copenhaver GP (2018) Meiotic Recombination: Mixing It Up in Plants. Annual
895 Review of Plant Biology 69:577–609. https://doi.org/10.1146/annurev-arplant-042817-
896 040431
897 Wang Y, Magnard JL, McCormick S, Yang M (2004) Progression through meiosis I and
898 meiosis II in arabidopsis anthers is regulated by an A-type cyclin predominately

899 expressed in prophase I. Plant Physiology 136:4127–4135.
900 https://doi.org/10.1104/pp.104.051201
901 Wang Y, Yang M (2014) Loss-of-function mutants and overexpression lines of the
902 arabidopsis cyclin CYCA1;2/TARDY asynchronous meiosis exhibit different defects in
903 prophase-I meiocytes but produce the same meiotic products. PLoS ONE 9:1–8.
904 https://doi.org/10.1371/journal.pone.0113348
905 Wijnker E, Harashima H, Müller K, Parra-Nuñez P, Bastiaan de Snoo C, van de Belt J,
906 Dissmeyer N, Bayer M, Pradillo M, Schnittger A (2019) The Cdk1/Cdk2 homolog
907 CDKA;1 controls the recombination landscape in Arabidopsis. Proceedings of the
908 National Academy of Sciences of the United States of America 116:12534–12539.
909 https://doi.org/10.1073/pnas.1820753116
910 Wijnker E, Schnittger A (2013) Control of the meiotic cell division program in plants. Plant
911 Reproduction 26:143–158. https://doi.org/10.1007/s00497-013-0223-x
912 Xu H, Luo X, Qian J, Pang X, Song J, Qian G, Chen J, Chen S (2012) FastUniq: A Fast De
913 Novo Duplicates Removal Tool for Paired Short Reads. PLoS ONE 7:1–6.
914 https://doi.org/10.1371/journal.pone.0052249
915 Yang C, Sofroni K, Wijnker E, Hamamura Y, Carstens L, Harashima H, Stolze SC, Vezon D,
916 Chelysheva L, Orban-Nemeth Z, Pochon G, Nakagami H, Schlögelhofer P, Grelon M,
917 Schnittger A (2020) The Arabidopsis Cdk1/Cdk2 homolog CDKA ;1 controls
918 chromosome axis assembly during plant meiosis . The EMBO Journal 39:1–19.
919 https://doi.org/10.15252/embj.2019101625
920 Yang F, Fernández-Jiménez N, Tučková M, Vrána J, Cápal P, Díaz M, Pradillo M, Pecinka A
921 (2021) Defects in meiotic chromosome segregation lead to unreduced male gametes in
922 Arabidopsis SMC5/6 complex mutants. Plant Cell 33:3104–3119.
923 https://doi.org/10.1093/plcell/koab178
924 Younis A, Hwang YJ, Lim KB (2014) Exploitation of induced 2n-gametes for plant breeding.
925 Plant Cell Reports 33:215–223. https://doi.org/10.1007/s00299-013-1534-y
926 Zhang XZ, Liu GJ, Yan LY, Zhao YB, Chang RF, Wu LP (2003) Creating triploid
927 germplasm via induced 2n pollen in Capsicum annuum L. Journal of Horticultural
928 Science and Biotechnology 78:84–88. https://doi.org/10.1080/14620316.2003.11511592
929 Zhou Q, Cheng X, Kong B, Zhao Y, Li Z, Sang Y, Wu J, Zhang P (2022) Heat shock-
930 induced failure of meiosis I to meiosis II transition leads to 2n pollen formation in a
931 woody plant. Plant Physiology. https://doi.org/10.1093/plphys/kiac219
932 Zinn KE, Tunc-Ozdemir M, Harper JF (2010) Temperature stress and plant sexual

933 reproduction: Uncovering the weakest links. Journal of Experimental Botany 61:1959–
934 1968. https://doi.org/10.1093/jxb/erq053
935
936

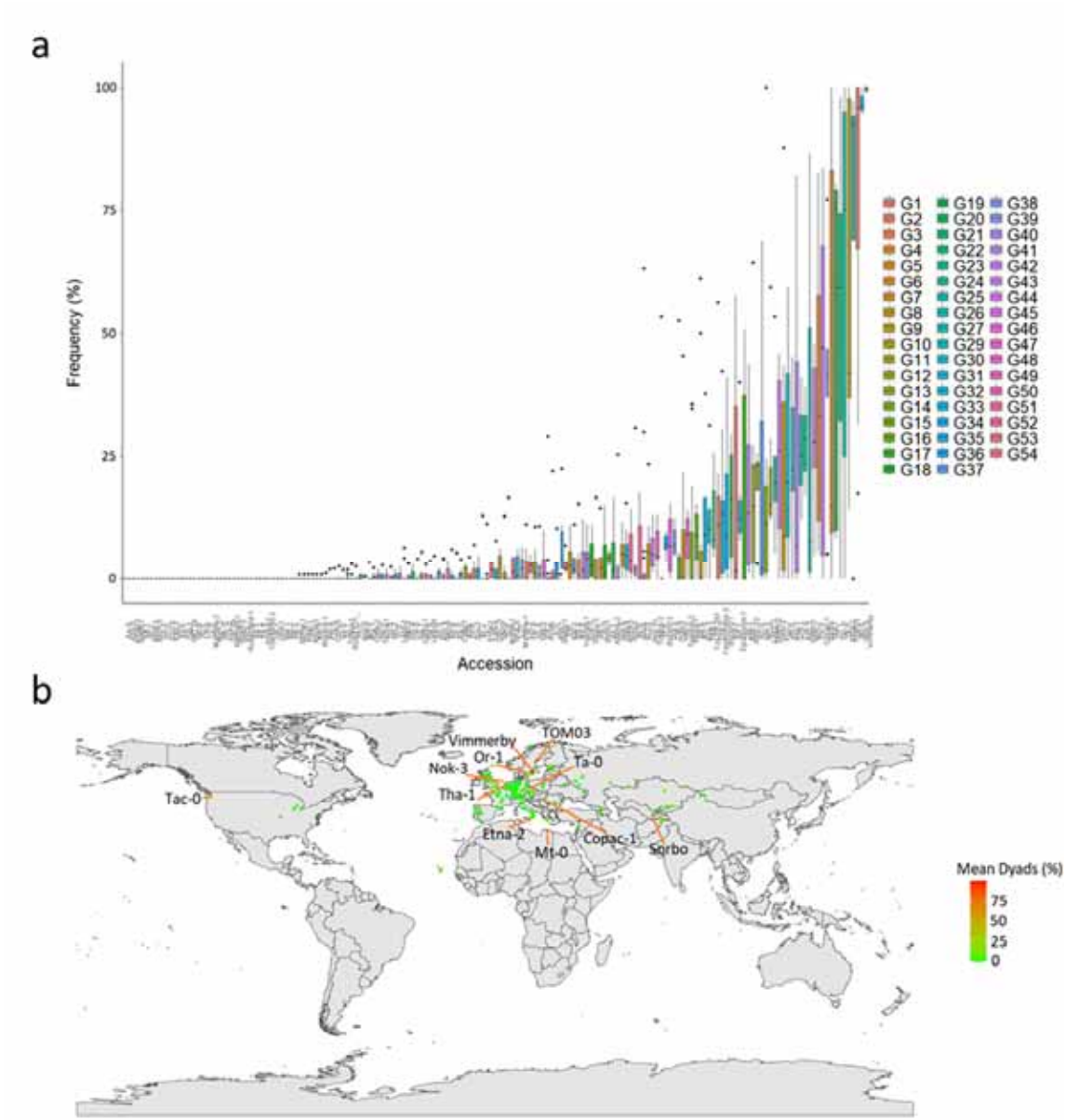

Figure 1 Natural variation in Arabidopsis heat induced meiotic restitution
a) Frequency of dyad production after 24h at 32°C for all 172 accessions analysed, ranked according to average dyad frequency. Boxes are coloured according to the batch the accession was analysed in (G1-G54). Lower and upper hinges of the box correspond to the first and third quartile. Whiskers extend from the hinges no further than 1.5 times the inter-quartile range (or to the highest or lowest data point). Data points beyond the range of the whiskers are plotted separately. **b)** Geographical location of the analysed accessions, coloured according to the average amount of dyads produced at the tetrad-stage after 24h at 32°C. The 11 highest dyad producing accessions are denoted with their name.

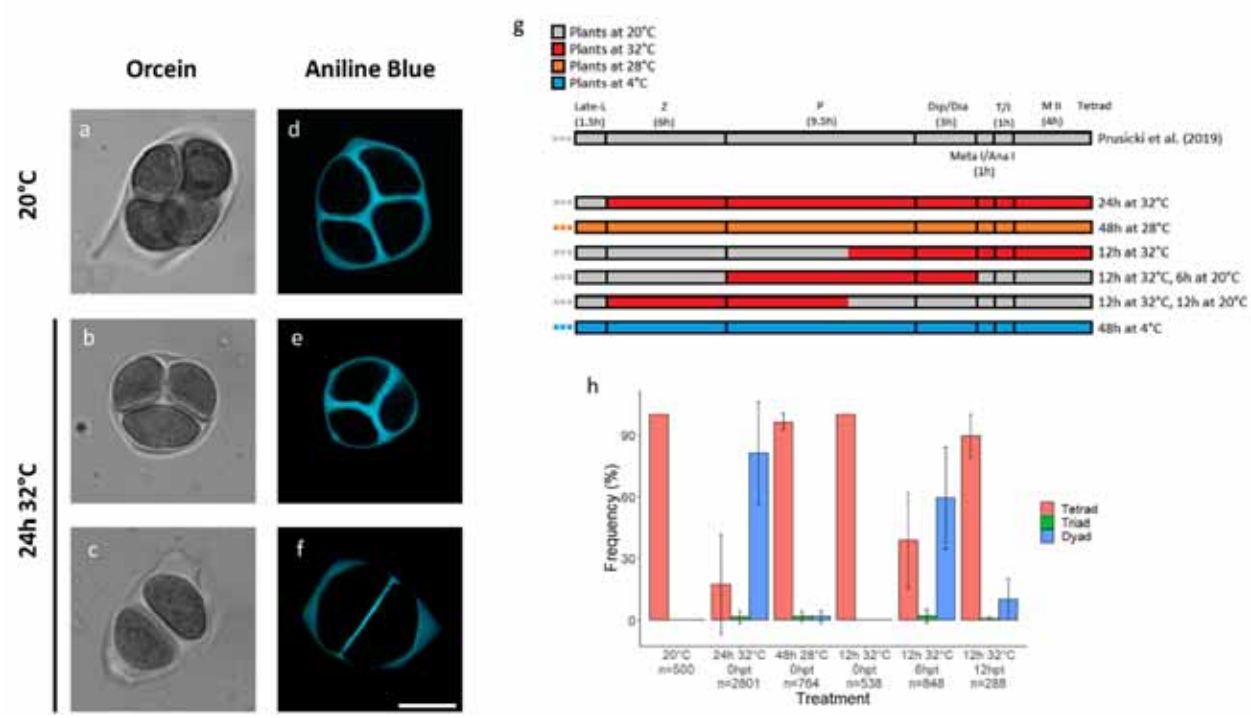

Figure 2 Mt-0 as the model for high dyad producers after heat.
Orcein **(a-c)** and aniline blue **(d-f)** stained Mt-0 tetrad-stage male meiocytes under control conditions **(a, d)** and after a 24h at 32°C heat treatment **(b, e, c, f)**. Scale bar = 10µm. **g)** Schematic overview of the different temperature treatments and durations applied to Mt-0 in regards to the timing and progression of male meiosis as described by Prusicki et al. (2019). **h)** Frequency (%) of the different configurations (tetrads, triads or dyads) observed at the tetrad-stage of Mt-0 after various temperature treatments. n represents the number of individual meiocytes counted. Error bars represent standard errors. A minimum of 3 plants were analysed for every treatment.

960

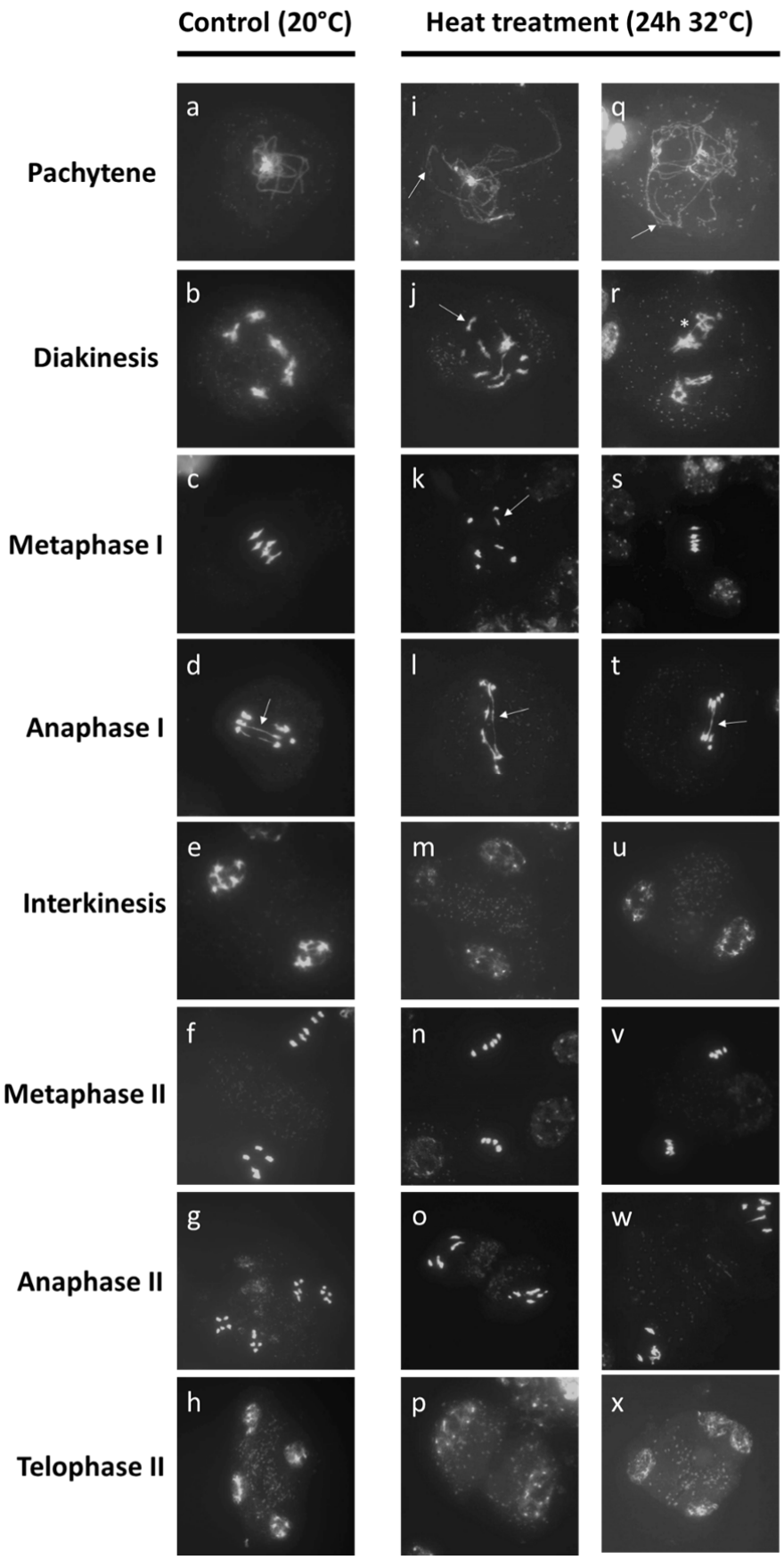
Control (20°C)
Heat treatment (24h 32°C)
Pachytene
Diakinesis
Metaphase I
Anaphase I
Interkinesis
Metaphase II
Anaphase II
Telophase II
a
b
c
d
e
f
g
h
i
j
k
l
m
n
o
p
q
r
s
t
u
v
w
x

961 **Figure 3** Meiotic spreads of Mt-0.
962 DAPI stained, enzyme digested chromosome spreads of Mt-0 male meiocytes at various
963 developmental stages under control conditions (20°C; **a-h**) and after a 24h at 32°C heat
964 treatment **(i-x)**. Regions of asynapsis at pachytene, univalents at diakinesis and metaphase I
965 and ectopic chromosome strands at anaphase I are indicated by arrows. Aberrant interactions
966 between non-homologous chromosomes at diakinesis are indicated with an asterix. Scale bar
967 = 10µm.
968

Female	Male Mt-0	Vimmerby	Ta-0	Tac-0	Etna-2	Or-1	Nok-3	Tha-1	Ler
Mt-0	81+-25	76+-47	73+-17	96+-7	61+-?	69+-29	98+-6	50+-3	3+-3
Vimmerby	-	100+-1	-	-	-	-	-	-	-
Ta-0	-	93+-6	51+-42	62+-35	-	-	-	-	-
Tac-0	-	91+-14	-	54+-34	-	-	-	-	-
Etna-2	-	97+-5	-	-	58+-38	-	-	-	-
Or-1	-	-	-	-	-	45+-34	-	-	-
Nok-3	-	-	-	-	-	-	77+-32	-	-
Tha-1	-	-	-	-	-	-	-	43+-43	-
Ler	-	9+-6	4+-4	6+-10	1+-1	1+-1	1+-2	5+-3	1+-1

Figure 4 Using Mt-0 and Ler as tester lines for heat induced meiotic restitution.
Dyad frequency at the tetrad-stage after 24h at 32°C for different F1 hybrids between several high dyad producing accessions and the Mt-0 and Ler tester lines. The diagonal represents the values for the individual natural accessions. Values are presented as the average dyad frequency +- standard deviation. Data were collected from at least 3 individual F1 plants per cross, except for the cross Mt-0xEtna-2 from which only 1 plant was available.

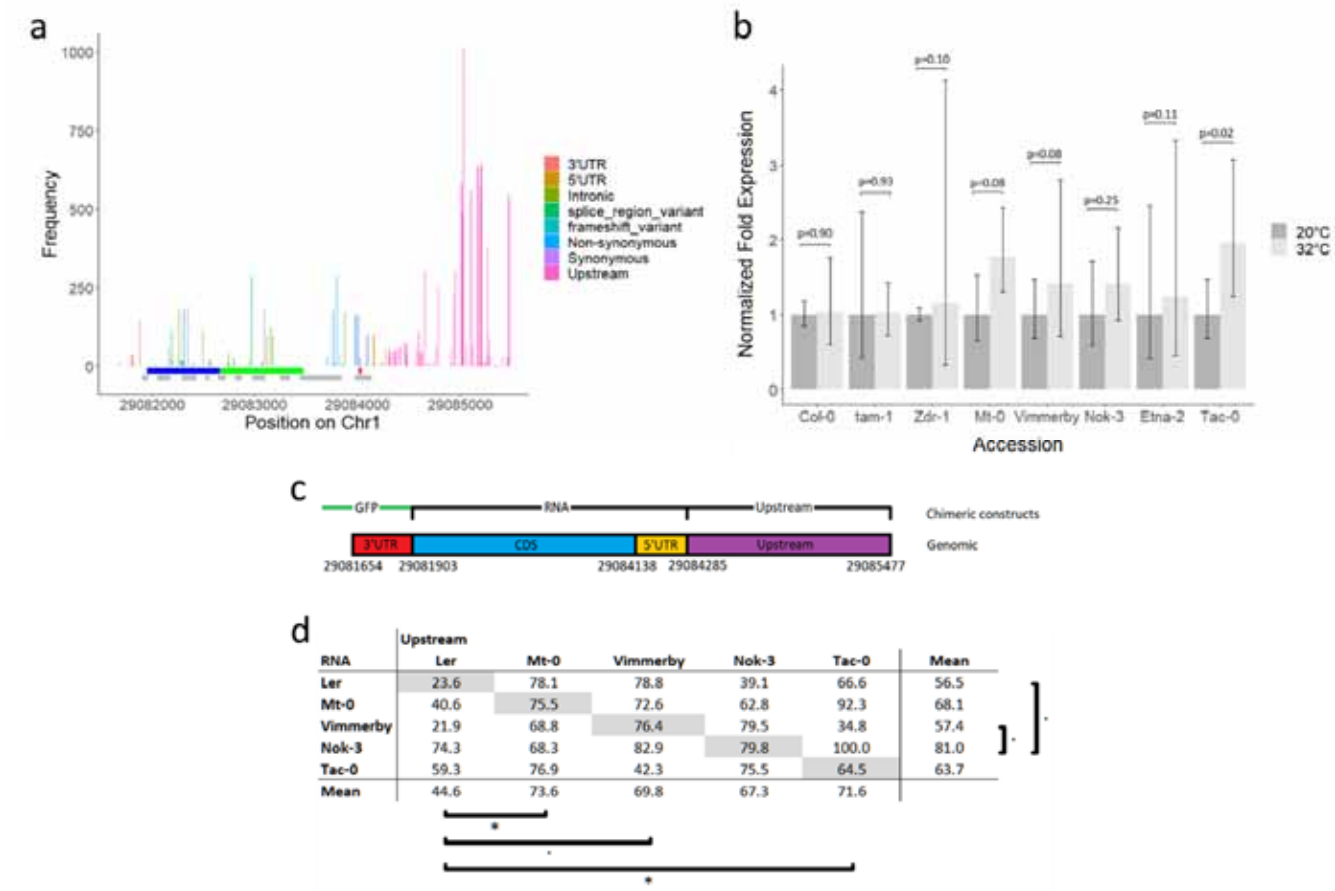

Figure 5 TAM/CYCA1;2 expression is influenced by temperature in the high dyad producing accessions.

a) SNP frequencies across the genomic positions of the TAM/CYCA1;2 locus. The frequency represents the number of accessions in the 1001 genomes project (Alonso-Blanco et al. 2016) that contain a SNP or indel at a certain position, compared to the Col-0 reference sequence. The blue, green and red horizontal bars represent the genomic positions of respectively the C-terminal and N-terminal cyclin domains and the D-box domain. The grey horizontal bars represent the positions of protein coding regions. **b)** RT-qPCR based TAM/CYCA1;2 expression levels from flowerbuds of plants grown at 20°C or after a 24h at 32°C heat treatment. Data are normalized to the 20°C control within each accession. Three individual plants were analysed per accession and per treatment. P-values correspond to a linear model fit comparing the 20°C control to the 32°C treatment within each accession. Error bars represent standard errors. **c)** Graphical representation of the TAM/CYCA1;2 genomic locus and the corresponding regions that were cloned from 5 different accessions to make chimeric constructs with a C-terminal GFP tag. Numbers represent the position on chromosome 1. **d)** Dyad frequency at the tetrad-stage after 24h at 32°C for different chimeric constructs of upstream and RNA genomic regions of 5 natural accessions transformed into the heat sensitive tam-1 mutant background. Data represent the average dyad frequency for at least 5 individual T1 plants. Statistical comparison of different upstream or RNA regions was done using a two-way ANOVA model, followed by Tukey corrected, post-hoc pairwise comparisons. '*' means $p<0.05$, '.' means $p<0.1$, all other pairwise comparisons are not shown.

1003

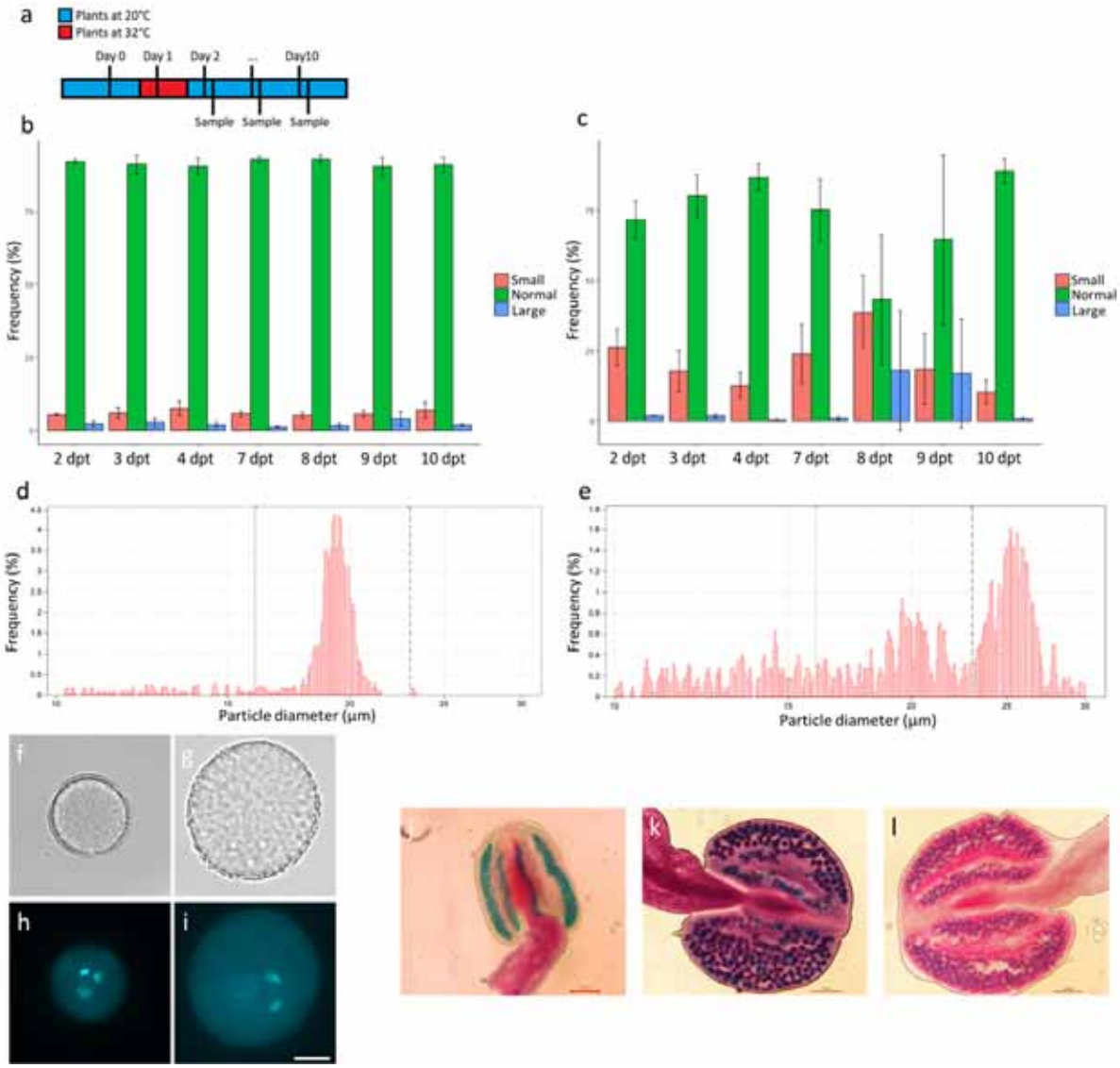

Figure 6 Heat induces restituted pollen formation in Mt-0.
a) Schematic overview of the 24h at 32°C heat treatment, return to the control condition growth rooms and subsequent flower sampling for Coulter Counter analysis. **b-c)** frequency (%) of small (10µm-16µm), normal (16µm-23µm) and large (23µm-30µm) pollen particles analysed through Coulter Counter analysis on 2-10 dpt for Mt-0 plants kept at control conditions (20°C; **b**) and plants heat treated for 24h at 32°C **(c)**. A minimum of 3 individual plants were analysed for every time point and treatment. Error bars represent standard errors. **d-e)** representative example of the pollen particle size distribution of Mt-0 plants kept at control conditions (20°C; **d**) and plants heat treated for 24h at 32°C **(e)**. The vertical dotted and dashed lines mark the particle sizes of 16µm and 23µm respectively. **f-i)** bright-field **(f, g)** and corresponding DAPI stained **(h, i)** images of control (20°C) pollen **(f, h)** and enlarged pollen of Mt-0 on day 9 after a 24h at 32°C heat treatment. Scale bar = 10µm. **j-l)** Alexander stained anthers of Mt-0 on days 3 **(j)**, 8 **(k)** and 10 **(l)** after a 24h at 32°C heat treatment. Scale bar = 100µm.

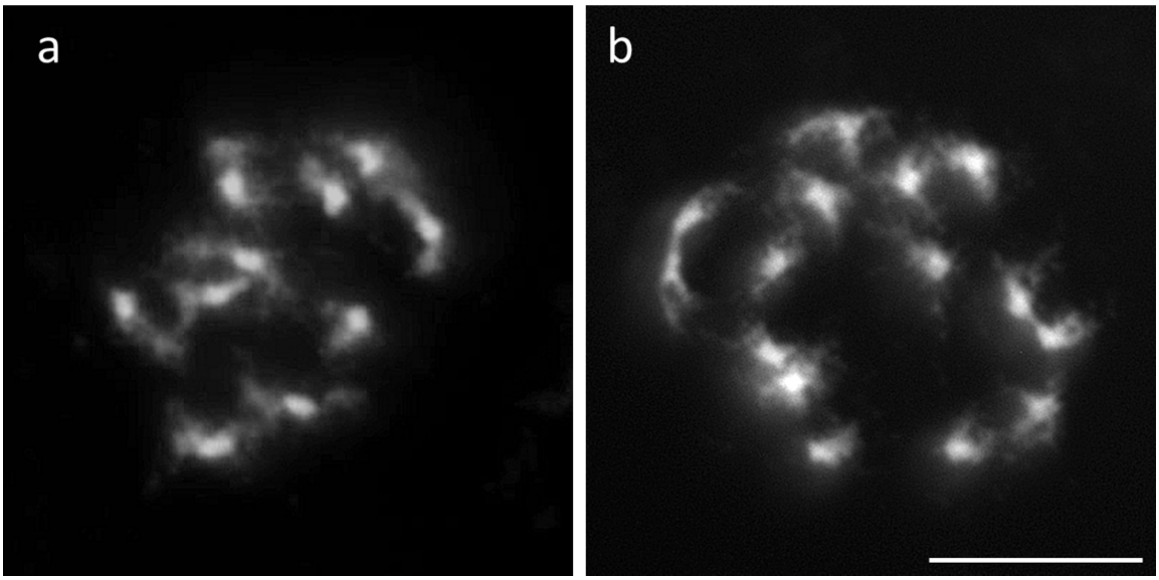

Figure 7 Chromosome spreads confirm the occurrence of triploid plants after heat in Mt-0. DAPI stained, enzyme digested mitotic chromosome spreads of a diploid (2n=10; **a**) and a triploid (3n=15; **b**) Mt-0 plant after heat treatment and self-fertilization. Scale bar = 10µm.

1028 **Table 1** TAM/CYCA1;2 expression is not likely affected by differential methylation under
1029 different temperatures.
1030 The frequency of methylated cytosines at SNP positions in the TAM/CYCA1;2 promotor of
1031 Col-0 vs Mt-0 at control conditions (20°C) or after a heat treatment of 24h at 32°C.
1032 Frequencies are shown as methylated on non-methylated plants for 3 biological replicates.
1033 The position is given relative to the 'A' in the 'ATG' start codon (A = position 0). NMS
1034 denotes the accession that carries No Methylation Site because of a different SNP. Missing
1035 data points are denoted by '-'.
1036

SNP Position	Col-0 20°C	Col-0 32°C	Mt-0 20°C	Mt-0 32°C
-16	0/3	0/3	NMS	NMS
-106	0/3	0/3	NMS	NMS
-109	0/3	0/3	NMS	NMS
-217	NMS	NMS	0/3	0/2
-246	NMS	NMS	0/3	0/2
-248	-	-	NMS	NMS
-627	0/3	0/3	NMS	NMS
-986	NMS	NMS	-	-

1037

1038 **Table 2** Triploid offspring after heat in accession Mt-0.
1039 The number of diploid (2n) and triploid (3n) plants recorded through flow cytometric analysis
1040 coming from a cross whereby Mt-0 after a 24h at 32°C heat treatment was either selfed, or
1041 used as the male or female parent in a cross with Mt-0 kept at 20°C. Seeds were harvested on
1042 siliques that were pollinated 8 or 9 days after the treatment (dpt). 'Germ' denotes the ratio of
1043 germinated on sown seeds.

Female Parent	Male Parent	8dpt			9dpt		
		2n	3n	Germ	2n	3n	Germ
Mt-0 (24h 32°C; Selfed)		2	8	10/33	1	4	5/50
Mt-0 (24h 32°C)	**Mt-0 (20°C)**	17	0	17/51	44	0	44/51
Mt-0 (20°C)	**Mt-0 (24h 32°C)**	77	0	77/102	64	15	79/102

1044

1045

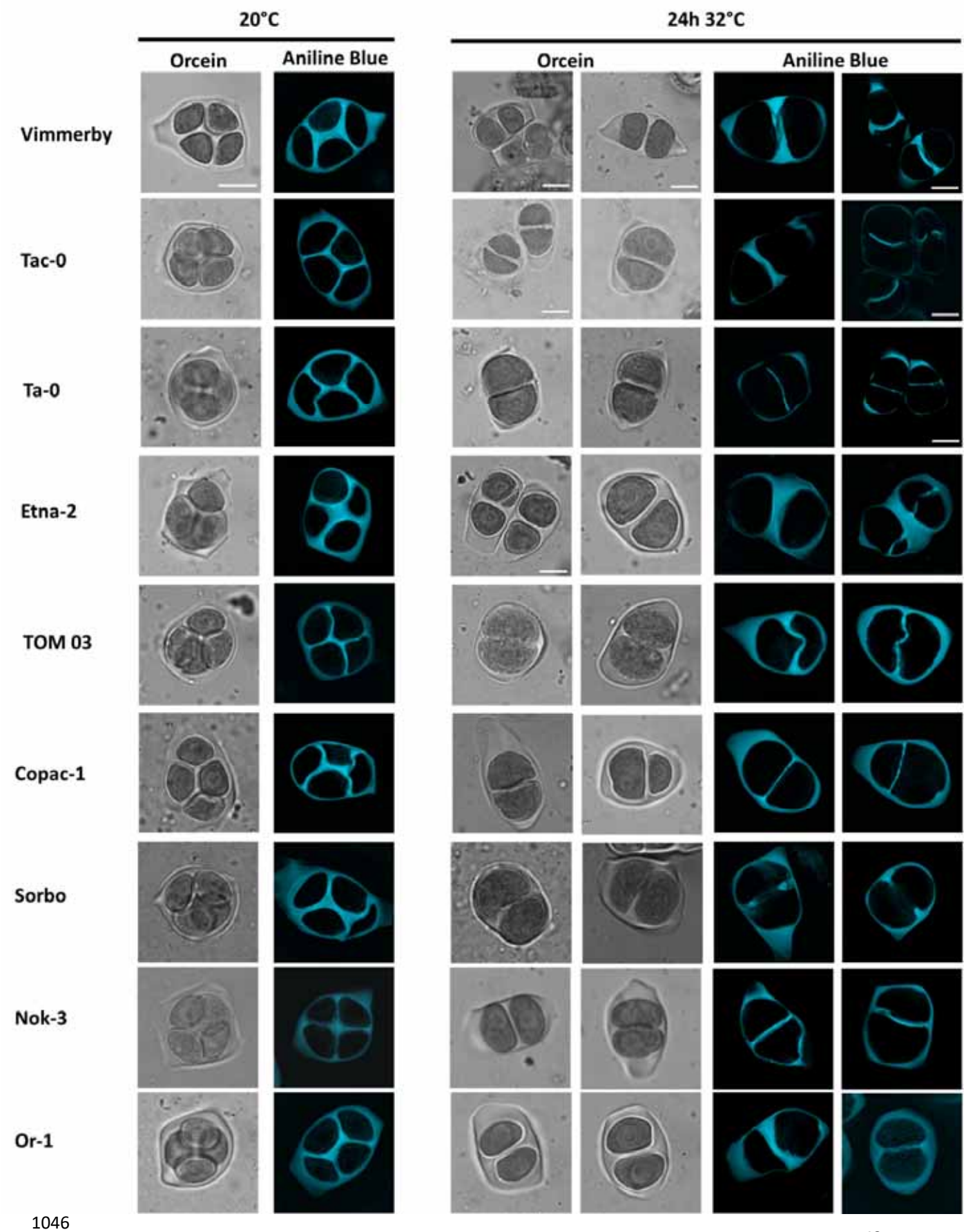
20°C
24h 32°C
Orcein
Aniline Blue
Orcein
Aniline Blue
Vimmerby
Tac-0
Ta-0
Etna-2
TOM 03
Copac-1
Sorbo
Nok-3
Or-1

1046

1047 **Supplemental Figure S1** High dyad after heat accessions' tetrad stage phenotype.
1048 Representative images of orcein or aniline blue stained tetrad-stage meiotic products of
1049 different high frequency, heat induced dyad producing accessions under control conditions
1050 (20°C) or immediately after a 24h at 32°C treatment. Scale bar = 10µm.
1051
1052

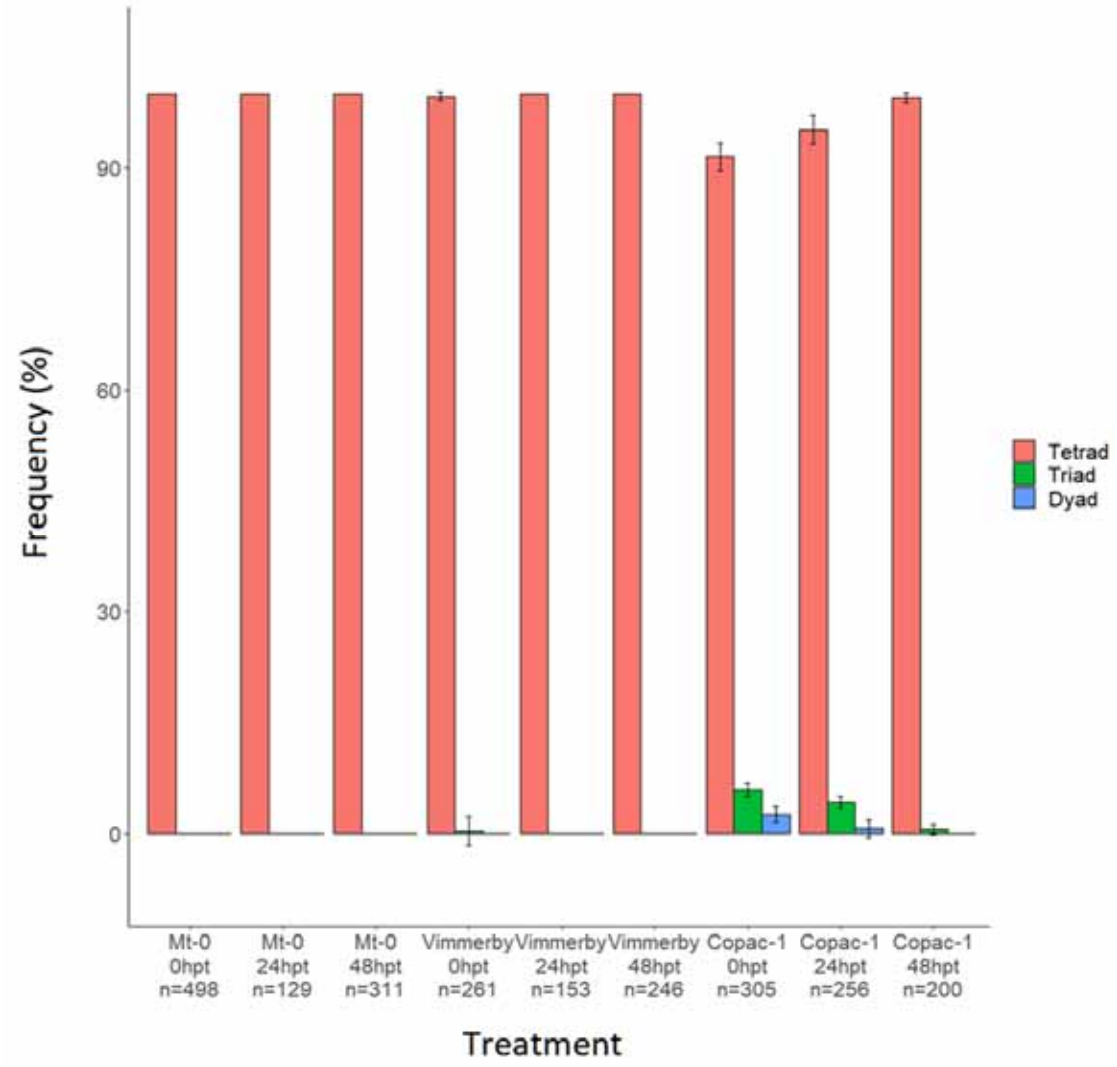

Supplemental Figure S2 The influence of cold on high dyads after heat producing accessions.

Frequency (%) of the different configurations (tetrads, triads or dyads) observed at the tetrad-stage of 3 high frequency, heat induced dyad producing accessions (Mt-0, Vimmerby and Copac-1) after a 48h at 4°C cold treatment on 0h, 24h or 48h after the treatment (hpt). Error bars represent standard errors, n represents the number of individual meiocytes counted.

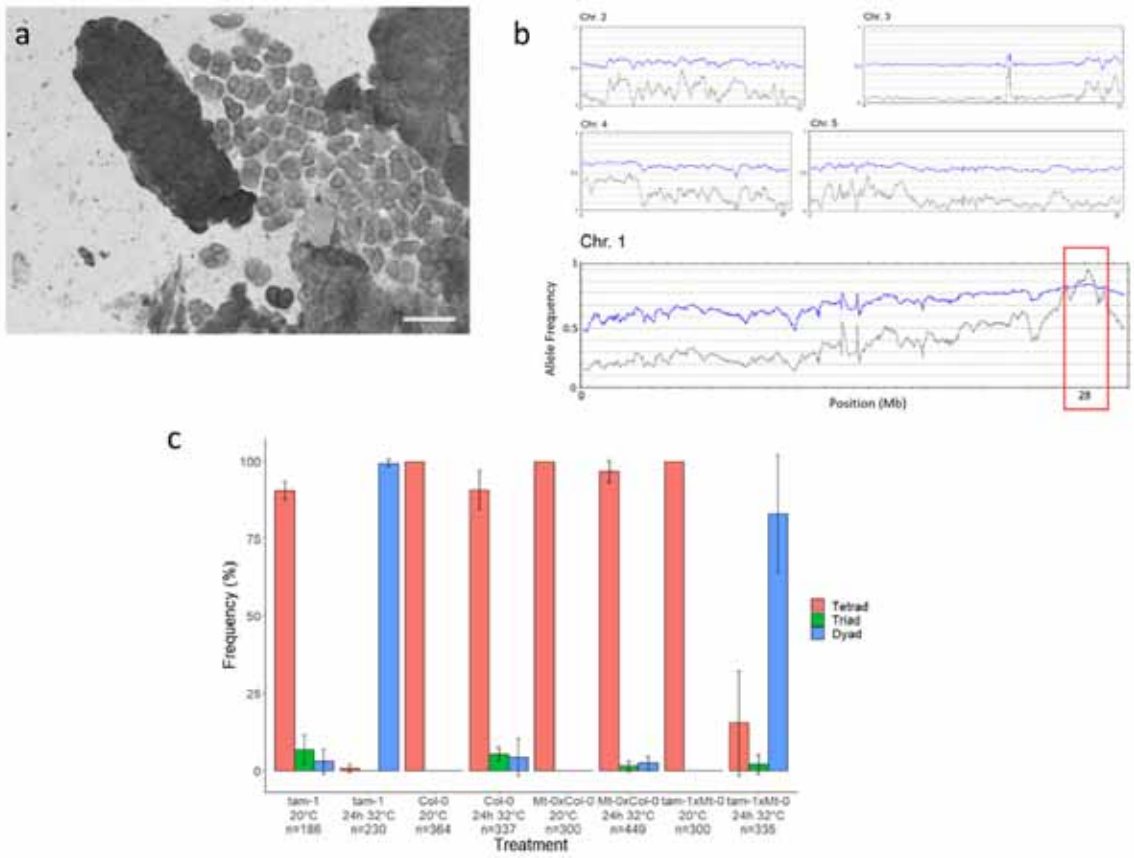

Supplemental Figure S3 Mapping of the Mt-0 locus.
a) Orcein stained tetrad-stage meiocytes of the Mt-0xLer heterozygous F1 show very few dyads after a 24h at 32°C heat treatment. Scale bar = 50µm. **b)** Allele frequency plot of the mapping population for the high dyad phenotype after heat stress of Mt-0xLer, analysed using SHOREmap V3.0. The blue line shows the average allele frequency within a 400kb window (5kb step size), the grey line follows the boost-values. The red rectangle denotes the predicted 2.4Mbp mapping interval. **c)** Frequency (%) of the different configurations (tetrads, triads or dyads) observed at the tetrad-stage of tam-1, Col-0, and the heterozygous Mt-0xCol-0 and tam-1xMt-0 F1s under control conditions (20°C) and after a 24h at 32°C heat treatment. n represents the number of individual meiocytes counted. Error bars represent standard errors. A minimum of 3 plants were analysed for every treatment.

Supplemental Figure S4 Methylation pattern of the TAM/CYCA1;2 promotor.
Excerpt from the 1001 epigenomes browser (http://neomorph.salk.edu/1001.aj.php) showing the methylation pattern of the TAM/CYCA1;2 (AT1G77390) promotor region. Data are included for 8 high frequency, heat induced dyad producing accessions (Vimmerby, Nok-3, Etna-2, Tac-0, Ta-0, Or-1, Tha-1, Mt-0) and for 12 of the lowest frequency dyad producing accessions (Col-0, Ler-0, Litva, Zdr-1, Angit-1, RRS-7, Angel-1, Di-G, Bsch-0, Uod-1, Gel-1, Tol-0).

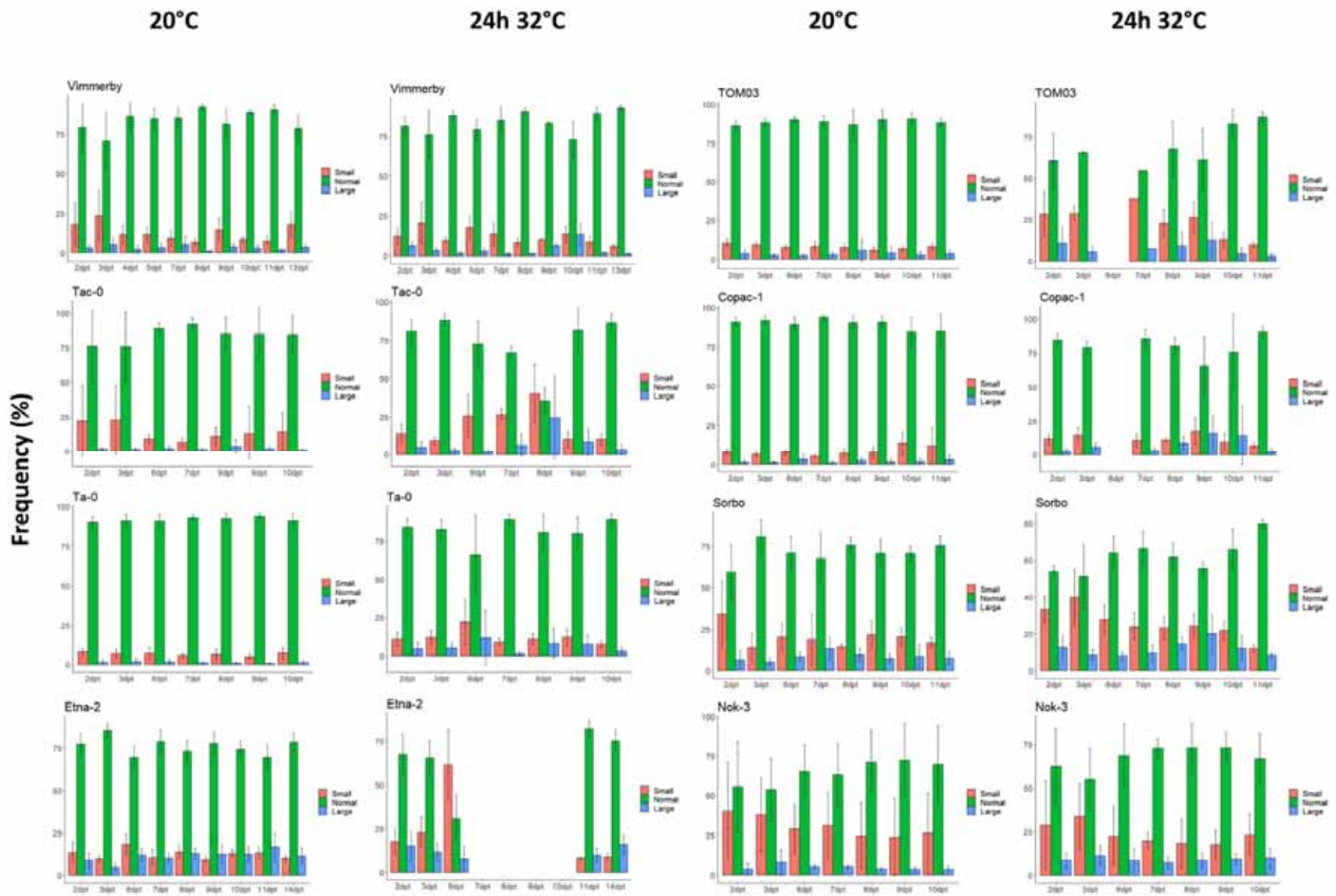
20°C
24h 32°C
20°C
24h 32°C
Frequency (%)
Vimmerby
Vimmerby
TOM03
TOM03
Tac-0
Tac-0
Copac-1
Copac-1
Ta-0
Ta-0
Sorbo
Sorbo
Etna-2
Etna-2
Nok-3
Nok-3
Small
Normal
Large

1091

1092 **Supplemental Figure S5** Pollen particle size time series for 8 high dyad after heat producing accessions.
1093 Frequency (%) of small (10µm-16µm), normal (16µm-23µm) and large (23µm-30µm) pollen particles analysed through Coulter Counter
1094 analysis for plants kept at control conditions (20°C) and plants heat treated for 24h at 32°C for 8 high dyad after heat producing accessions. A
1095 minimum of 3 individual plants were analysed for every time point and treatment. Error bars represent standard errors. dpt = days after the heat
1096 treatment.
1097
1098

1099

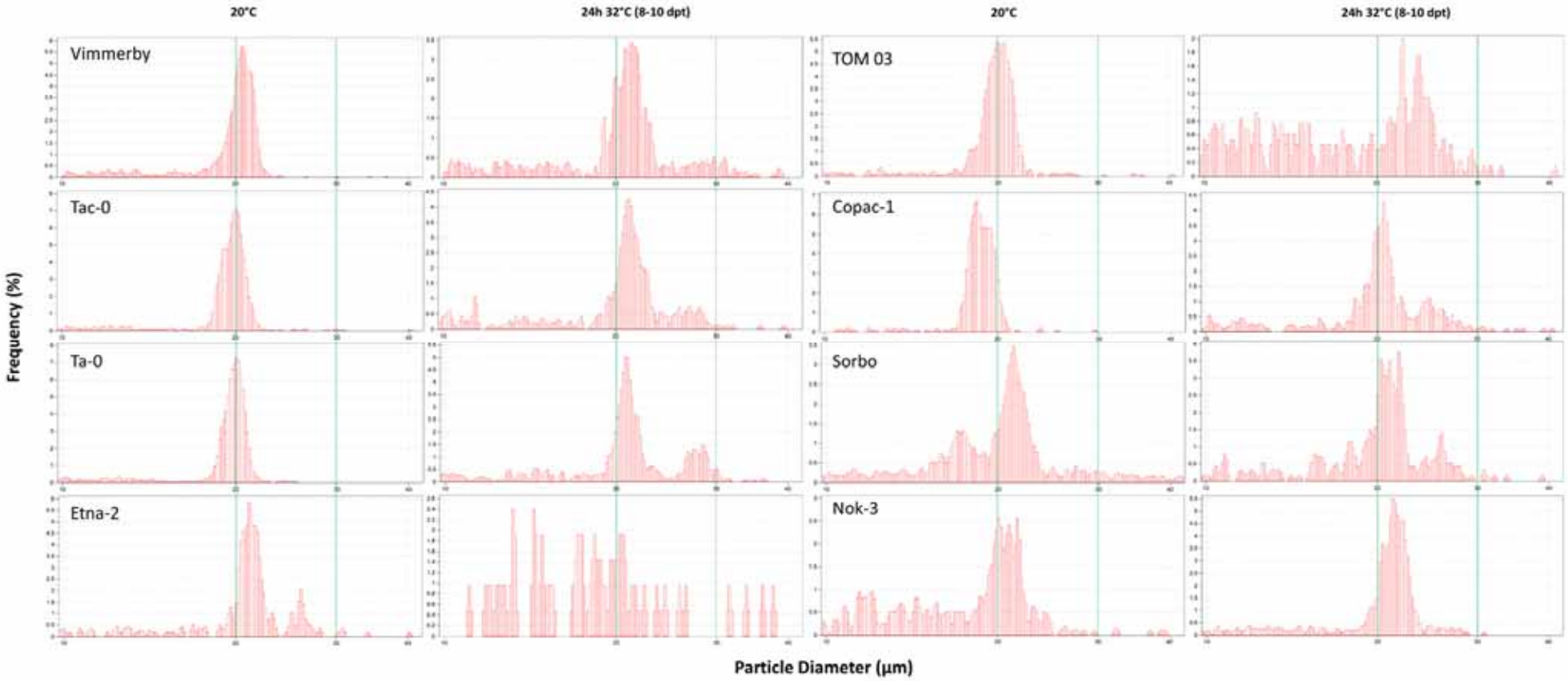
20°C
24h 32°C (8-10 dpt)
20°C
24h 32°C (8-10 dpt)
Vimmerby
TOM 03
Tac-0
Copac-1
Ta-0
Sorbo
Etna-2
Nok-3
Frequency (%)
Particle Diameter (µm)

1100 **Supplemental Figure S6** Pollen particle size distribution for 8 high dyad after heat producing accessions.
1101 Examples of the pollen particle size distributions of 8 high dyad after heat producing accessions for plants kept at control conditions (20°C) and
1102 plants heat treated for 24h at 32°C. The vertical green lines mark the particle sizes of 20µm and 30µm for easy comparison.
1103
1104

1105 **Supplemental Table S1** Quantification of callose wall phenotypes for multiple accessions.
1106 Counts of the number of dyads (after 24h at 32°C) or tetrads (after 20°C) having callose walls
1107 of normal, sturdy or thin thickness (based on visual inspection of aniline blue stained
1108 meiocytes) of several high frequency, heat induced dyad producing accessions. Major
1109 fractions are denoted in bold. n represents the number of individual tetrads or dyads counted.
1110

	n		Normal		Sturdy		Thin	
	20°C	**24h 32°C**	**20°C**	**24h 32°C**	**20°C**	**24h 32°C**	**20°C**	**24h 32°C**
Mt-0	21	34	**21**	9	0	0	0	**25**
Vimmerby	19	35	**19**	2	0	**33**	0	0
Etna-2	7	16	**6**	1	1	**13**	0	2
Tac-0	40	27	**40**	1	0	9	0	**17**
Ta-0	12	30	**12**	0	0	0	0	**30**
TOM03	33	29	**33**	2	0	**27**	0	0
Copac-1	23	58	**23**	5	0	0	0	**53**
Sorbo	33	14	**33**	0	0	0	0	**14**
Nok-3	26	8	**26**	1	0	0	0	**7**
Or-1	26	32	**26**	6	0	**15**	0	11

1111

1112 **Supplemental Table S2** Quantifications of nuclei per cell at the tetrad stage.
1113 Counts of the number of cells containing 1, 2 or more nuclei in dyads of several high
1114 frequency, heat induced dyad producing accessions (based on visual inspection of orcein
1115 stained meiocytes) after 24h at 32°C. Both cells in a dyad were counted separately.
1116

	1 Nucleus	2 Nuclei	More
Mt-0	34	0	0
Vimmerby	41	15	0
Ta-0	26	6	0
Tac-0	17	1	0
Or-1	50	0	0
Etna-2	30	4	0
TOM03	35	7	0
Copac-1	17	15	0
Sorbo	10	14	0
Nok-3	3	11	0

1117

1118 **Supplemental Table S3** Quantification of balanced and unbalanced meiocytes at the tetrad
1119 stage.
1120 Counts of the number of balanced and unbalanced dyads after 24h at 32°C for several high
1121 frequency, heat induced dyad producing accessions. In a balanced dyad the 2 cells appear to
1122 be equal size, in an unbalanced dyad 1 of the cells is a lot larger than the other (based on
1123 visual inspection of aniline blue and orcein stained meiocytes).
1124

	Balanced	Unbalanced
Mt-0	51	0
Vimmerby	63	0
Ta-0	38	8
Tac-0	33	3
Or-1	57	0
Etna-2	33	0
TOM03	50	0
Copac-1	39	57
Sorbo	22	4
Nok-3	14	1

1125

1126 **Supplemental Table S4** Analysis of the segregation pattern of the Mt-0 locus.
1127 Observed and expected number of individual plants for a 1:3 ratio of low (<5%) vs high
1128 (>>5%) heat-induced dyads at the tetrad-stage of a segregating F2 population of a cross
1129 between Mt-0 and Ler. The chi-squared value, degrees of freedom (df) and p-value
1130 correspond to a goodness-of-fit test between the observed and expected values.
1131

	<5% dyads	**>>5% dyads**	**Total**
Observed	730	201	931
Expected (1:3)	698	233	931
chi-squared	5.77		
df	1		
p-value	0.016		

1132

1133 **Supplemental Table S5** Primers used in this study.
1134

Name	Sequence	Purpose
TAM_WGS_F3	CATCACCCATTGCG TGAGAG	Genotyping tam-1
TAM_WGS_R3	AATCCTGGTTCATTAAGGCAA G	Genotyping tam-1
EF1aA4-qRT-F	AGGCTGGTATCTCTAAGGATGGTCA	qPCR
EF1aA4-qRT-R	GGATTTTGTCAGGGTTGTATCCG	qPCR
TAM_qPCR_F	ACTCTCATCTGATGTGGTTGC	qPCR
TAM_qPCR_R(rvc)	AAAGCTCTTGCGGTAGTGAC	qPCR
pTAM_gDNAPromotorR4R1_F	GGGGACAACTTTGTATAGAAAAGTTGTAagagttagagcacgcggtg	Promotor Cloning
pTAM_gDNAPromotorR4R1_R	GGGGACTGCTTTTTTGTACAAACTTGTgttttctttgattaggggttttctattttatatttattataagaa	Promotor Cloning
pTAM_gDNAPromotorR4R1_R_Mt-0SNPs	GGGGACTGCTTTTTTGTACAAACTTGTgttttctttgattaggggttttctttttttctatttattataagaa	Promotor Cloning (Mt-0 specific)
pTAM_gDNAPromotorR4R1_F_Nok-3_Tac-0SNPs	GGGGACAACTTTGTATAGAAAAGTTGTAagggttacagcacgcggtg	Promotor Cloning (Nok-3 and Tac-0 specific)
TAM_gDNA5'UTR_R1R2_F	GGGGACAAGTTTGTACAAAAAAGCAGGCTTAaaaataattccgcgtttttcattttccgt	RNA region Cloning
TAM_gDNAR1R2_noSTOP_R	GGGGACCACTTTGTACAAGAAAGCTGGGTTgaggaaaagctcttgcggtagtg	RNA region Cloning
TAM_gDNA5'UTR_R1R2_F_Mt-0	GGGGACAAGTTTGTACAAAAAAGCAGGCTTAaaaatgattccgcgtttttcattttccgt	RNA region Cloning (Mt-0 specific)
Col_BAS_F3	TAGGAATTGAAAAAGGAATAAAAAGTAG	Bisulfite PCR (Col-0 specific)
Col_BAS_R3	AAAATAAAAAACCCCTAATCAAAAAAAA	Bisulfite PCR (Col-0 specific)
Col_BAS_F5	TGGAAATTTGATTTAATTTTTTTTGAGT	Bisulfite PCR (Col-0 specific)
Col_BAS_R5	CTTCTACAACTACTATATCATCTACTTC	Bisulfite PCR (Col-0 specific)
Mt-0_BAS_F6	ATATTGTTGATGAAGTAATGGAAAATTT	Bisulfite PCR (Mt-0 specific)
Mt-0_BAS_R6	TACTCTTATTTAAACCCTCTAAAATACA	Bisulfite PCR (Mt-0 specific)
Mt-0_BAS_F8	AGTAAATTTTTTTTGTATTTTAGAGGGT	Bisulfite PCR (Mt-0 specific)
Mt-0_BAS_R8	ATATCCTTCTACAACTACTATATCATCT	Bisulfite PCR (Mt-0 specific)

Parsed Citations

Ahmed M, Kim DR (2018) pcr: An R package for quality assessment, analysis and testing of qPCR data. PeerJ 2018:. https://doi.org/10.7717/peerj.4473
Google Scholar: Author Only Title Only Author and Title

Alexander MP (1969) Differential staining of aborted and nonaborted pollen. Stain technology 44:117–122. https://doi.org/10.3109/10520296909063335
Google Scholar: Author Only Title Only Author and Title

Alonso-Blanco C, Andrade J, Becker C, Bemm F, Bergelson J, Borgwardt KMM, Cao J, Chae E, Dezwaan TMM, Ding W, Ecker JRR, Exposito-Alonso M, Farlow A, Fitz J, Gan X, Grimm DGG, Hancock AMM, Henz SRR, Holm S, et al (2016) 1,135 Genomes Reveal the Global Pattern of Polymorphism in Arabidopsis thaliana. Cell 166:481–491. https://doi.org/10.1016/j.cell.2016.05.063
Google Scholar: Author Only Title Only Author and Title

Andreuzza S, Nishal B, Singh A, Siddiqi I (2015) The Chromatin Protein DUET/MMD1 Controls Expression of the Meiotic Gene TDM1 during Male Meiosis in Arabidopsis. PLoS Genetics 11:1–22. https://doi.org/10.1371/journal.pgen.1005396
Google Scholar: Author Only Title Only Author and Title

Andrews S, Krueger F, Seegonds-Pichon A, Biggins L, Krueger C, Wingett S (2014) FastQC: a quality control tool for high throughput sequence data. In: FastQC: a quality control tool for high throughput sequence data. http://www.bioinformatics.babraham.ac.uk/projects/fastqc. Accessed 5 Oct 2020
Google Scholar: Author Only Title Only Author and Title

Bac-Molenaar JA, Fradin EF, Becker FFM, Rienstra JA, van der Schoot J, Vreugdenhil D, Keurentjes JJB (2015) Genome-wide association mapping of fertility reduction upon heat stress reveals developmental stage-specific QTLs in Arabidopsis Thaliana. Plant Cell 27:1857–1874. https://doi.org/10.1105/tpc.15.00248
Google Scholar: Author Only Title Only Author and Title

Bloom JS, Boocock J, Treusch S, Sadhu MJ, Day L, Oates-Barker H, Kruglyak L (2019) Rare variants contribute disproportionately to quantitative trait variation in yeast. eLife 8:1–19. https://doi.org/10.7554/eLife.49212
Google Scholar: Author Only Title Only Author and Title

Bolger AM, Lohse M, Usadel B (2014) Trimmomatic: A flexible trimmer for Illumina sequence data. Bioinformatics 30:2114–2120. https://doi.org/10.1093/bioinformatics/btu170
Google Scholar: Author Only Title Only Author and Title

Bomblies K, Higgins JD, Yant L (2015) Meiosis evolves: Adaptation to external and internal environments. New Phytologist 208:306–323. https://doi.org/10.1111/nph.13499
Google Scholar: Author Only Title Only Author and Title

Brennan RS, Garrett AD, Huber KE, Hargarten H, Pespeni MH (2019) Rare genetic variation and balanced polymorphisms are important for survival in global change conditions. Proceedings of the Royal Society B: Biological Sciences 286:. https://doi.org/10.1098/rspb.2019.0943
Google Scholar: Author Only Title Only Author and Title

Bretagnolle F, Thompson JD (1995) Gametes with the somatic chromosome number: mechanisms of their formation and role in the evolution of autopolyploid plants. New Phytologist 129:1–22. https://doi.org/10.1111/j.1469-8137.1995.tb03005.x
Google Scholar: Author Only Title Only Author and Title

Brownfield L, Köhler C (2011) Unreduced gamete formation in plants: Mechanisms and prospects. Journal of Experimental Botany 62:1659–1668. https://doi.org/10.1093/jxb/erq371
Google Scholar: Author Only Title Only Author and Title

Brownfield L, Yi J, Jiang H, Minina EA, Twell D, Köhler C (2015) Organelles maintain spindle position in plant meiosis. Nature Communications 6:. https://doi.org/10.1038/ncomms7492
Google Scholar: Author Only Title Only Author and Title

Bulankova P, Riehs-Kearnan N, Nowack MK, Schnittger A, Riha K (2010) Meiotic progression in Arabidopsis is governed by complex regulatory interactions between SMG7, TDM1, and the meiosis I-specific cyclin TAM. Plant Cell 22:3791–3803. https://doi.org/10.1105/tpc.110.078378
Google Scholar: Author Only Title Only Author and Title

Chaturvedi P, Wiese AJ, Ghatak A, Záveská Drábková L, Weckwerth W, Honys D (2021) Heat stress response mechanisms in pollen development. New Phytologist 231:571–585. https://doi.org/10.1111/nph.17380
Google Scholar: Author Only Title Only Author and Title

Chen Y, Müller F, Rieu I, Winter P (2016) Epigenetic events in plant male germ cell heat stress responses. Plant Reproduction 29:21–29. https://doi.org/10.1007/s00497-015-0271-5
Google Scholar: Author Only Title Only Author and Title

Cifuentes M, Jolivet S, Cromer L, Harashima H, Bulankova P, Renne C, Crismani W, Nomura Y, Nakagami H, Sugimoto K, Schnittger A, Riha K, Mercier R (2016) TDM1 Regulation Determines the Number of Meiotic Divisions. PLoS Genetics 12:1–22. https://doi.org/10.1371/journal.pgen.1005856
Google Scholar: Author Only Title Only Author and Title

Cromer L, Heyman J, Touati S, Harashima H, Araou E, Girard C, Horlow C, Wassmann K, Schnittger A, de Veylder L, Mercier R (2012) OSD1 promotes meiotic progression via APC/C inhibition and forms a regulatory network with TDM and CYCA1;2/TAM. PLoS Genetics 8:. https://doi.org/10.1371/journal.pgen.1002865
Google Scholar: Author Only Title Only Author and Title

d'Erfurth I, Cromer L, Jolivet S, Girard C, Horlow C, Sun Y, To JPC, Berchowitz LE, Copenhaver GP, Mercier R (2010) The CYCLIN-A CYCA1;2/TAM is required for the meiosis I to meiosis II transition and cooperates with OSD1 for the prophase to first meiotic division transition. PLoS Genetics 6:1–12. https://doi.org/10.1371/journal.pgen.1000989
Google Scholar: Author Only Title Only Author and Title

d'Erfurth I, Jolivet S, Froger N, Catrice O, Novatchkova M, Mercier R (2009) Turning meiosis into mitosis. PLoS Biology 7:. https://doi.org/10.1371/journal.pbio.1000124
Google Scholar: Author Only Title Only Author and Title

d'Erfurth I, Jolivet S, Froger N, Catrice O, Novatchkova M, Simon M, Jenczewski E, Mercier R (2008) Mutations in AtPS1 (Arabidopsis thaliana Parallel Spindle 1) lead to the production of diploid pollen grains. PLoS Genetics 4:1–9. https://doi.org/10.1371/journal.pgen.1000274
Google Scholar: Author Only Title Only Author and Title

De Jaeger-Braet J, Krause L, Buchholz A, Schnittger A (2022) Heat stress reveals a specialized variant of the pachytene checkpoint in meiosis of Arabidopsis thaliana . The Plant Cell 34:433–454. https://doi.org/10.1093/plcell/koab257
Google Scholar: Author Only Title Only Author and Title

De Storme N, Copenhaver GP, Geelen D (2012) Production of diploid male gametes in Arabidopsis by cold-induced Destabilization of postmeiotic radial microtubule arrays. Plant Physiology 160:1808–1826. https://doi.org/10.1104/pp.112.208611
Google Scholar: Author Only Title Only Author and Title

De Storme N, Geelen D (2014) The impact of environmental stress on male reproductive development in plants: Biological processes and molecular mechanisms. Plant, Cell and Environment 37:1–18. https://doi.org/10.1111/pce.12142
Google Scholar: Author Only Title Only Author and Title

De Storme N, Geelen D (2013) Cytokinesis in plant male meiosis. Plant Signaling and Behavior 8:. https://doi.org/10.4161/psb.23394
Google Scholar: Author Only Title Only Author and Title

De Storme N, Geelen D (2020) High temperatures alter cross-over distribution and induce male meiotic restitution in Arabidopsis thaliana. Communications Biology 3:1–15. https://doi.org/10.1038/s42003-020-0897-1
Google Scholar: Author Only Title Only Author and Title

De Storme N, Geelen D (2011) The arabidopsis mutant jason produces unreduced first division restitution male gametes through a parallel/ fused spindle mechanism in meiosis II. Plant Physiology 155:1403–1415. https://doi.org/10.1104/pp.110.170415
Google Scholar: Author Only Title Only Author and Title

De Storme N, Zamariola L, Mau M, Sharbel TF, Geelen D (2013) Volume-based pollen size analysis: An advanced method to assess somatic and gametophytic ploidy in flowering plants. Plant Reproduction 26:65–81. https://doi.org/10.1007/s00497-012-0209-0
Google Scholar: Author Only Title Only Author and Title

Deng Y, Srivastava R, Quilichini TD, Dong H, Bao Y, Horner HT, Howell SH (2016) IRE1, a component of the unfolded protein response signaling pathway, protects pollen development in Arabidopsis from heat stress. Plant Journal 88:193–204. https://doi.org/10.1111/tpj.13239
Google Scholar: Author Only Title Only Author and Title

Fox DT, Soltis DE, Soltis PS, Ashman TL, Van de Peer Y (2020) Polyploidy: A Biological Force From Cells to Ecosystems. Trends in Cell Biology 30:688–694. https://doi.org/10.1016/j.tcb.2020.06.006
Google Scholar: Author Only Title Only Author and Title

Galbraith DW, Harkins KR, Maddox JM, Ayres NM, Sharma DP, Firoozabady E (1983) Rapid flow cytometric analysis of the cell cycle in intact plant tissues. Science 220:1049–1051. https://doi.org/10.1126/science.220.4601.1049
Google Scholar: Author Only Title Only Author and Title

Giorno F, Wolters-Arts M, Mariani C, Rieu I (2013) Ensuring reproduction at high temperatures: The heat stress response during anther and pollen development. Plants 2:489–506. https://doi.org/10.3390/plants2030489
Google Scholar: Author Only Title Only Author and Title

Jeffrey PD, Russo AA, Polyak K, Gibbs E, Hurwitz J, Massagué J, Pavletich NP (1995) Mechanism of CDK activation revealed by the structure of a cyclinA-CDK2 complex. Nature 376:313–320
Google Scholar: Author Only Title Only Author and Title

Johnson-Brousseau SA, McCormick S (2004) A compendium of methods useful for characterizing Arabidopsis pollen mutants and gametophytically-expressed genes. Plant Journal 39:761–775. https://doi.org/10.1111/j.1365-313X.2004.02147.x
Google Scholar: Author Only Title Only Author and Title

Kawakatsu T, Huang S shan C, Jupe F, Sasaki E, Schmitz RJJ, Urich MAA, Castanon R, Nery JRR, Barragan C, He Y, Chen H, Dubin M, Lee CR, Wang C, Bemm F, Becker C, O'Neil R, O'Malley RCC, Quarless DXX, et al (2016) Epigenomic Diversity in a Global Collection of Arabidopsis thaliana Accessions. Cell 166:492–505. https://doi.org/10.1016/j.cell.2016.06.044
Google Scholar: Author Only Title Only Author and Title

Kosmacz M, Gorka M, Schmidt S, Luzarowski M, Moreno JC, Szlachetko J, Leniak E, Sokolowska EM, Sofroni K, Schnittger A, Skirycz A (2019) Protein and metabolite composition of Arabidopsis stress granules. New Phytologist 222:1420–1433. https://doi.org/10.1111/nph.15690
Google Scholar: Author Only Title Only Author and Title

Lardon R, Wijnker E, Keurentjes J, Geelen D (2020) The genetic framework of shoot regeneration in Arabidopsis comprises master regulators and conditional fine-tuning factors. Communications Biology 3:1–13. https://doi.org/10.1038/s42003-020-01274-9
Google Scholar: Author Only Title Only Author and Title

Lee YS, Maple R, Dürr J, Dawson A, Tamim S, del Genio C, Papareddy R, Luo A, Lamb JC, Amantia S, Sylvester AW, Birchler JA, Meyers BC, Nodine MD, Rouster J, Gutierrez-Marcos J (2021) A transposon surveillance mechanism that safeguards plant male fertility during stress. Nature Plants 7:34–41. https://doi.org/10.1038/s41477-020-00818-5
Google Scholar: Author Only Title Only Author and Title

Li Y, Huang Y, Sun H, Wang T, Ru W, Pan L, Zhao X, Dong Z, Huang W, Jin W (2022) Heat shock protein 101 contributes to the thermotolerance of male meiosis in maize. The Plant Cell
Google Scholar: Author Only Title Only Author and Title

Li Y, Shen Y, Cai C, Zhong C, Zhu L, Yuan M, Ren H (2010) The type II Arabidopsis formin14 interacts with microtubules and microfilaments to regulate cell division. Plant Cell 22:2710–2726. https://doi.org/10.1105/tpc.110.075507
Google Scholar: Author Only Title Only Author and Title

Lloyd A, Morgan C, Franklin FCH, Bomblies K (2018) Plasticity of meiotic recombination rates in response to temperature in arabidopsis. Genetics 208:1409–1420. https://doi.org/10.1534/genetics.117.300588
Google Scholar: Author Only Title Only Author and Title

Lokker AC, Barba-Gonzalez R, Lim KB, Ramanna MS, Van Tuyl JM (2005) Genotypic and environmental variation in production of 2n-gametes of oriental x asiatic lily hybrids. Acta Horticulturae 673:453–456. https://doi.org/10.17660/ActaHortic.2005.673.58
Google Scholar: Author Only Title Only Author and Title

Magnard J, Yang M, Chen YS, Leary M, Mccormick S (2001) Required for the Normal Pace and Synchrony of Cell Division during Male Meiosis 1. Society 127:1157–1166. https://doi.org/10.1104/pp.010473.1
Google Scholar: Author Only Title Only Author and Title

Malik S (2022) Epigenetic Regulation of Heat Stress in Plant Male Reproduction. Frontiers in Plant Science 13:. https://doi.org/10.3389/fpls.2022.826473
Google Scholar: Author Only Title Only Author and Title

Mercier R, Mézard C, Jenczewski E, Macaisne N, Grelon M (2015) The Molecular Biology of Meiosis in Plants. Annual Review of Plant Biology 66:297–327. https://doi.org/10.1146/annurev-arplant-050213-035923
Google Scholar: Author Only Title Only Author and Title

Mittler R, Finka A, Goloubinoff P (2012) How do plants feel the heat? Trends in Biochemical Sciences 37:118–125. https://doi.org/10.1016/j.tibs.2011.11.007
Google Scholar: Author Only Title Only Author and Title

Modliszewski JL, Copenhaver GP (2017) Meiotic recombination gets stressed out: CO frequency is plastic under pressure. Current Opinion in Plant Biology 36:95–102. https://doi.org/10.1016/j.pbi.2016.11.019
Google Scholar: Author Only Title Only Author and Title

Monroe JG, Srikant T, Carbonell-Bejerano P, Becker C, Lensink M, Exposito-Alonso M, Klein M, Hildebrandt J, Neumann M, Kliebenstein D, Weng ML, Imbert E, Ågren J, Rutter MT, Fenster CB, Weigel D (2022) Mutation bias reflects natural selection in Arabidopsis thaliana. Nature 602:101–105. https://doi.org/10.1038/s41586-021-04269-6
Google Scholar: Author Only Title Only Author and Title

Morgan CH, Zhang H, Bomblies K (2017) Are the effects of elevated temperature on meiotic recombination and thermotolerance linked via the axis and synaptonemal complex? Philosophical Transactions of the Royal Society B: Biological Sciences 372:.

https://doi.org/10.1098/rstb.2016.0470
Google Scholar: Author Only Title Only Author and Title

Naydenov M, Baev V, Apostolova E, Gospodinova N, Sablok G, Gozmanova M, Yahubyan G (2015) High-temperature effect on genes engaged in DNA methylation and affected by DNA methylation in Arabidopsis. Plant Physiology and Biochemistry 87:102–108. https://doi.org/10.1016/j.plaphy.2014.12.022
Google Scholar: Author Only Title Only Author and Title

Ning Y, Liu Q, Wang C, Qin E, Wu Z, Wang M, Yang K, Elesawi IE, Chen C, Liu H, Qin R, Liu B (2021) Heat stress interferes with formation of double-strand breaks and homolog synapsis. Plant Physiology 185:1783–1797. https://doi.org/10.1093/plphys/kiab012
Google Scholar: Author Only Title Only Author and Title

Novikova PY, Hohmann N, Van de Peer Y (2018) Polyploid Arabidopsis species originated around recent glaciation maxima. Current Opinion in Plant Biology 42:8–15. https://doi.org/10.1016/j.pbi.2018.01.005
Google Scholar: Author Only Title Only Author and Title

Omidi M, Siahpoosh MR, Mamghani R, Modarresi M (2014) The influence of terminal heat stress on meiosis abnormalities in pollen mother cells of wheat. Cytologia 79:49–58. https://doi.org/10.1508/cytologia.79.49
Google Scholar: Author Only Title Only Author and Title

Osman K, Higgins JD, Sanchez-Moran E, Armstrong SJ, Franklin FCH (2011) Pathways to meiotic recombination in Arabidopsis thaliana. New Phytologist 190:523–544. https://doi.org/10.1111/j.1469-8137.2011.03665.x
Google Scholar: Author Only Title Only Author and Title

Pécrix Y, Rallo G, Folzer H, Cigna M, Gudin S, Le Bris M (2011) Polyploidization mechanisms: Temperature environment can induce diploid gamete formation in Rosa sp. Journal of Experimental Botany 62:3587–3597. https://doi.org/10.1093/jxb/err052
Google Scholar: Author Only Title Only Author and Title

Prelich G (2012) Gene overexpression: Uses, mechanisms, and interpretation. Genetics 190:841–854. https://doi.org/10.1534/genetics.111.136911
Google Scholar: Author Only Title Only Author and Title

Protter DSW, Parker R (2016) Principles and Properties of Stress Granules. Trends in Cell Biology 26:668–679. https://doi.org/10.1016/j.tcb.2016.05.004
Google Scholar: Author Only Title Only Author and Title

Prusicki MA, Keizer EM, Van Rosmalen RP, Komaki S, Seifert F, Müller K, Wijnker E, Fleck C, Schnittger A (2019) Live cell imaging of meiosis in arabidopsis thaliana. eLife 8:1–31. https://doi.org/10.7554/eLife.42834
Google Scholar: Author Only Title Only Author and Title

Qi F, Zhang F (2020) Cell Cycle Regulation in the Plant Response to Stress. Frontiers in Plant Science 10:1–10. https://doi.org/10.3389/fpls.2019.01765
Google Scholar: Author Only Title Only Author and Title

Rieu I, Twell D, Firon N (2017) Pollen development at high temperature: From acclimation to collapse. Plant Physiology 173:1967–1976. https://doi.org/10.1104/pp.16.01644
Google Scholar: Author Only Title Only Author and Title

Ross KJ, Fransz P, Jones GH (1996) A light microscopic atlas of meiosis in Arabidopsis thaliana. Chromosome Research 4:507–516. https://doi.org/10.1007/BF02261778
Google Scholar: Author Only Title Only Author and Title

Schindfessel C, Drozdowska Z, De Mooij L, Geelen D (2021) Loss of obligate crossovers, defective cytokinesis and male sterility in barley caused by short-term heat stress. Plant Reproduction 34:243–253. https://doi.org/10.1007/s00497-021-00415-2
Google Scholar: Author Only Title Only Author and Title

Sofroni K, Takatsuka H, Yang C, Dissmeyer N, Komaki S, Hamamura Y, Böttger L, Umeda M, Schnittger A (2020) CDKD-dependent activation of CDKA;1 controls microtubule dynamics and cytokinesis during meiosis. Journal of Cell Biology 219:. https://doi.org/10.1083/JCB.201907016
Google Scholar: Author Only Title Only Author and Title

Sun H, Schneeberger K (2015) SHOREmap v3.0: Fast and Accurate Identifi cation of Causal Mutations from Forward Genetic Screens. In: Alonso JM, Stepanova AN (eds) Plant Functional Genomics: Methods and Protocols: Second Edition, 2nd editio. Springer, New York, pp 381–395
Google Scholar: Author Only Title Only Author and Title

Taylor SC, Nadeau K, Abbasi M, Lachance C, Nguyen M, Fenrich J (2019) The Ultimate qPCR Experiment: Producing Publication Quality, Reproducible Data the First Time. Trends in Biotechnology 37:761–774. https://doi.org/10.1016/j.tibtech.2018.12.002
Google Scholar: Author Only Title Only Author and Title

Tian M, Zhang Y, Liu Y, Kang X, Zhang P (2018) High temperature exposure did not affect induced 2n pollen viability in Populus. Plant Cell and Environment 41:1383–1393. https://doi.org/10.1111/pce.13165
Google Scholar: Author Only Title Only Author and Title

Van de Peer Y, Ashman TL, Soltis PS, Soltis DE (2021) Polyploidy: an evolutionary and ecological force in stressful times. The Plant cell 33:11–26. https://doi.org/10.1093/plcell/koaa015
Google Scholar: Author Only Title Only Author and Title

Vanneste K, Baele G, Maere S, Van De Peer Y (2014) Analysis of 41 plant genomes supports a wave of successful genome duplications in association with the Cretaceous-Paleogene boundary. Genome Research 24:1334–1347. https://doi.org/10.1101/gr.168997.113
Google Scholar: Author Only Title Only Author and Title

Vergne P, Delvallee I, Dumas C (1987) Rapid assessment of microspore and pollen development stage in wheat and maize usind DAPI and membrane permeabilization. Stain technology 62:299–304. https://doi.org/10.1016/0960-0760(93)90156-Q
Google Scholar: Author Only Title Only Author and Title

Wainschtein P, Jain D, Zheng Z, Cupples LA, Shadyab AH, McKnight B, Shoemaker BM, Mitchell BD, Psaty BM, Kooperberg C, Liu CT, Albert CM, Roden D, Chasman DI, Darbar D, Lloyd-Jones DM, Arnett DK, Regan EA, Boerwinkle E, et al (2022) Assessing the contribution of rare variants to complex trait heritability from whole-genome sequence data. Nature genetics 54:263–273. https://doi.org/10.1038/s41588-021-00997-7
Google Scholar: Author Only Title Only Author and Title

Wang J, Li D, Shang F, Kang X (2017) High temperature-induced production of unreduced pollen and its cytological effects in Populus. Scientific Reports 7:1–12. https://doi.org/10.1038/s41598-017-05661-x
Google Scholar: Author Only Title Only Author and Title

Wang P, Zhou Z, Hu A, Pontede Albuquerque C, Zhou Y, Hong L, Sierecki E, Ajiro M, Kruhlak M, Harris C, Guan KL, Zheng ZM, Newton AC, Sun P, Zhou H, Fu XD (2014) Both decreased and increased SRPK1 levels promote cancer by interfering with PHLPP-mediated dephosphorylation of Akt. Molecular Cell 54:378–391. https://doi.org/10.1016/j.molcel.2014.03.007
Google Scholar: Author Only Title Only Author and Title

Wang Y, Copenhaver GP (2018) Meiotic Recombination: Mixing It Up in Plants. Annual Review of Plant Biology 69:577–609. https://doi.org/10.1146/annurev-arplant-042817-040431
Google Scholar: Author Only Title Only Author and Title

Wang Y, Magnard JL, McCormick S, Yang M (2004) Progression through meiosis I and meiosis II in arabidopsis anthers is regulated by an A-type cyclin predominately expressed in prophase I. Plant Physiology 136:4127–4135. https://doi.org/10.1104/pp.104.051201
Google Scholar: Author Only Title Only Author and Title

Wang Y, Yang M (2014) Loss-of-function mutants and overexpression lines of the arabidopsis cyclin CYCA1;2/TARDY asynchronous meiosis exhibit different defects in prophase-I meiocytes but produce the same meiotic products. PLoS ONE 9:1–8. https://doi.org/10.1371/journal.pone.0113348
Google Scholar: Author Only Title Only Author and Title

Wijnker E, Harashima H, Müller K, Parra-Nuñez P, Bastiaan de Snoo C, van de Belt J, Dissmeyer N, Bayer M, Pradillo M, Schnittger A (2019) The Cdk1/Cdk2 homolog CDKA;1 controls the recombination landscape in Arabidopsis. Proceedings of the National Academy of Sciences of the United States of America 116:12534–12539. https://doi.org/10.1073/pnas.1820753116
Google Scholar: Author Only Title Only Author and Title

Wijnker E, Schnittger A (2013) Control of the meiotic cell division program in plants. Plant Reproduction 26:143–158. https://doi.org/10.1007/s00497-013-0223-x
Google Scholar: Author Only Title Only Author and Title

Xu H, Luo X, Qian J, Pang X, Song J, Qian G, Chen J, Chen S (2012) FastUniq: A Fast De Novo Duplicates Removal Tool for Paired Short Reads. PLoS ONE 7:1–6. https://doi.org/10.1371/journal.pone.0052249
Google Scholar: Author Only Title Only Author and Title

Yang C, Sofroni K, Wijnker E, Hamamura Y, Carstens L, Harashima H, Stolze SC, Vezon D, Chelysheva L, Orban-Nemeth Z, Pochon G, Nakagami H, Schlögelhofer P, Grelon M, Schnittger A (2020) The Arabidopsis Cdk1/Cdk2 homolog CDKA;1 controls chromosome axis assembly during plant meiosis . The EMBO Journal 39:1–19. https://doi.org/10.15252/embj.2019101625
Google Scholar: Author Only Title Only Author and Title

Yang F, Fernández-Jiménez N, Tučková M, Vrána J, Cápal P, Díaz M, Pradillo M, Pecinka A (2021) Defects in meiotic chromosome segregation lead to unreduced male gametes in Arabidopsis SMC5/6 complex mutants. Plant Cell 33:3104–3119. https://doi.org/10.1093/plcell/koab178
Google Scholar: Author Only Title Only Author and Title

Younis A, Hwang YJ, Lim KB (2014) Exploitation of induced 2n-gametes for plant breeding. Plant Cell Reports 33:215–223.

https://doi.org/10.1007/s00299-013-1534-y
Google Scholar: Author Only Title Only Author and Title

Zhang XZ, Liu GJ, Yan LY, Zhao YB, Chang RF, Wu LP (2003) Creating triploid germplasm via induced 2n pollen in Capsicum annuum L. Journal of Horticultural Science and Biotechnology 78:84–88. https://doi.org/10.1080/14620316.2003.11511592
Google Scholar: Author Only Title Only Author and Title

Zhou Q, Cheng X, Kong B, Zhao Y, Li Z, Sang Y, Wu J, Zhang P (2022) Heat shock-induced failure of meiosis I to meiosis II transition leads to 2n pollen formation in a woody plant. Plant Physiology. https://doi.org/10.1093/plphys/kiac219
Google Scholar: Author Only Title Only Author and Title

Zinn KE, Tunc-Ozdemir M, Harper JF (2010) Temperature stress and plant sexual reproduction: Uncovering the weakest links. Journal of Experimental Botany 61:1959–1968. https://doi.org/10.1093/jxb/erq053
Google Scholar: Author Only Title Only Author and Title